12-2016

The Effect of Process Parameters and Surface Condition on Bond Strength between Additively Manufactured Components and Polymer Substrates

Bharat Bhushan Chivukula
University of Arkansas, Fayetteville

The Effect of Process Parameters and Surface Condition on Bond Strength between Additively Manufactured Components and Polymer Substrates

A thesis submitted in partial fulfillment
of the requirements for the degree of
Master of Science in Industrial Engineering

by

Bharat Bhushan Chivukula
Osmania University
Bachelor of Science in Mechanical Engineering, 2011

December 2016
University of Arkansas

This thesis is approved for recommendation to the Graduate Council.

____
Dr. Harry Pierson
Thesis Director

____
Dr. Haitao Liao
Committee Member

____
Dr. Manuel Rossetti
Committee Member

Abstract

Additive patching is a process in which printers with multiple axes deposit molten material onto a pre-defined surface to form a bond. Studying the effect of surface roughness and process parameters selected for printing auxiliary part on the bond helps in improving the strength of the final component. Particularly, the influence of surface roughness, as established by adhesion theory, has not been evaluated in the framework of additive manufacturing (AM). A full factorial design of experiments with five replications was conducted on two levels and three factors, viz., layer thickness, surface roughness, and raster angle to examine the underlying effects on bond strength. Analysis of variance (ANOVA) was used to test the resultant index and distributions were plotted to analyze various conditions. Experimental results indicated that bond strength increased up to 27% at higher surface roughness and lower layer thickness levels. Full factorial experiments with additional levels were conducted to realize the direction of improvement and find optimum values of layer thickness and surface roughness. It was found that at a layer thickness of 0.1 mm and 502.94 µin of surface roughness bond strength attains the highest value. This research represents a first step towards understanding bond strength in patching/re-manufacturing, allowing manufacturers to intelligently select process parameters for the production of both the substrate and the added geometry.

Acknowledgements

I am grateful to Dr. Harry Pierson for giving an opportunity to work with him. The guidance and support provided by him was necessary to complete this research work.

I would like to thank Dr. Liao and Dr. Manuel D. Rossetti for their inputs in improving this work. I am thankful to my research group in Automation lab for their help in setting up machines and also for contributing valuable ideas to improve research. Special thanks to Dr. Bernhardt, Mark L. Kuss and fellow colleagues Matthew Watters & Behdad Mofarraj in Civil Engineering for their help in using mechanics laboratory.

This thesis is dedicated to my parents, who helped me become the person I am today. I would like to thank them for all their love during my good and bad times. Thank you for believing and supporting my decision to pursue higher studies. I thank my brother Krishna Kishore for all his guidance in every phase of my life to help me walk in the path of success. Also, I would like to thank that person who instigated the thought to fly here without which I would have never had a chance to write this page.

Table of Contents

List of Tables

List of Figures

1. Introduction

Additive manufacturing (AM) is a bottom-up layering process to fabricate parts based on a computer aided design (CAD) model. Parts designed using CAD software are sliced into layers. AM is also known as 3D printing and used in industry to produce prototypes and end products with complex geometries, which are difficult to manufacture using conventional subtractive manufacturing approaches. 3D printing allows manufacturers to modify designs rapidly, thus reducing costs at each product development stage. The prototypes can also be tested rapidly, thereby reducing the time to market a product (Piazza & Alexander, 2015). Fused filament fabrication (FFF) is one of the 3D printing processes which is widely available and used in many industries for making prototypes, conducting academic research, and fabricating consumer goods. In FFF, the plastic material is heated to a semi-molten state and deposited onto a pre-heated build plate. An extruder nozzle that moves according to tool path (G-code) generated by slicing software deposits molten material on top of the existing layer. Forced convection and heat dissipation by conduction bond the deposited material with the existing layer (Zhang & Chou, 2006).

Although AM offers flexibility in design and fabrication, its widespread adoption in manufacturing is limited by technological challenges. One of these challenges is the inability of the printer to build overhanging structures in the absence of support structures, which leads to wastage of material and fabrication time. Mechanical strength is anisotropic, being lower in the Z-direction; layers stacked in the vertical direction have less mechanical strength than materials in the plane of these layers (Oropallo & Piegl, 2016). Furthermore, the speed of 3D printers is considerably slower than traditional manufacturing processes, which makes them impractical for high-volume production.

Poor surface finish is another major problem that affects the functionality of AM parts. The surface profile of the part resembles a rectangle-type staircase (Ahn, Kweon, Kwon, Song, & Lee, 2009). This is called the stair stepping effect and can be visualized clearly on inclined and curved surfaces as shown in Figure 1.1.

Layer thickness and build orientation are two important that affect the mechanical strength as well as the dimensional accuracy of AM structures (Sood, Ohdar, & Mahapatra, 2009). Reducing layer thickness reduces stair stepping, but increases the number of layers to print, thereby increasing the printing time and cost. Increasing layer thickness can reduce the time to build parts however, it increases the surface roughness. Build orientation also affects the surface quality of a part. Orienting a part that has certain angles parallel to the build direction (XY plane) can reduce the stair stepping effect (Oropallo *et al.*, 2016).

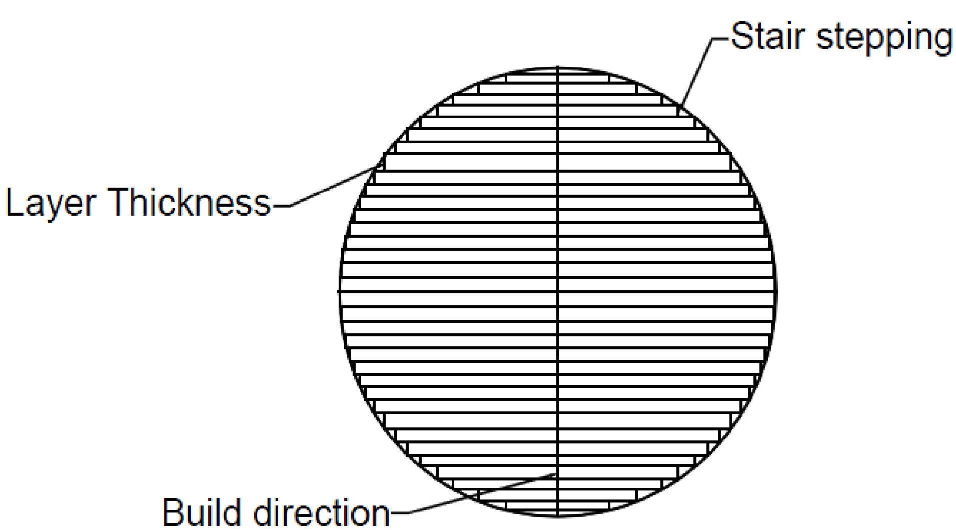

Figure 1.1. Stair Stepping effect in layered printing

Recent research suggests a growing interest to alleviate the drawbacks of AM such as 5- and 6- axis printing, remanufacturing AM workpieces, and printing on injection molded enclosures that contain active components. Printing with 5- or 6- axis machines can improve surface finish, eliminate anisotropic properties, reduce the need for support material, and aid in printing on curved surfaces. Grutle (2016), in his thesis work, built a 5-axis printing machine which rotated the workpiece and added material to the print from different directions. Adding an extra axis to the printer solved some of the major limitations of 3D printers as discussed earlier. Since the machine rotated the workpiece, the need for support material was eliminated, thereby reducing the time and cost to print the part. Also, the surface finish of the parts printed using 5-axis machine at layer thicknesses of 0.1, 0.2, and 0.4 mm showed improvement compared to the parts printed using a conventional 3D printer. The main advantage of the 5-axis printer was the ability to control print direction, which permitted strategic alignment of property anisotropies. Song, Pan, & Chen (2015), in their paper, developed a 6-axis system for multi-direction printing which enables 6 degrees of freedom between the tool and the workpiece. This system is particularly adept at building on or around inserts and other pre-made components. A multi-functional compound fabrication platform was introduced by Keating & Oxman (2013) to perform additive, formative, and subtractive fabrication. The 3D printing system utilized additional axes to deposit material on pre-existing, complex 3D surfaces and reduced the printing time as the process started on an existing print rather than blank build platform. Building parts in any direction was possible without the need for support material. The new approach improved the strength, surface finish, material utilization, and printing cost.

Considerable effort has been directed towards increasing the efficiency of 3D printing by minimizing the time and material consumed via introduction of patching and re-printing processes. Since engineering design is an iterative process, last minute changes may occur even after finalizing a design. Traditionally, AM parts cannot be reworked. If the part is not satisfactory, either due to a process failure or a judgement that additional design iteration is required, the part is discarded and a new version is fabricated from scratch. The introduction of patching or re-printing in AM process solves this problem by providing flexibility to print on an existing part, thereby reducing material wastage and printing time. Teibrich *et al*. (2015) worked on a patching system that integrated 5-axis printing, scanning, and milling into a single device to remanufacture an existing print using subtractive and additive manufacturing process. A dual-axis rotating platform was added to the Maker-gear Replicator-2 3D printer for the provision of two additional axes. This allowed patching geometry along different directions and reduced material consumption by eliminating the need for support material. Patching in different directions allows the anisotropic properties in a part to be oriented advantageously, hence providing better strength. Krassenstein (2014), in his report, discussed printing on top of an existing part. An affordable 3D scanning system was fixed on top of the printer to detect the pose of the part that was printed on the print bed. Polylactic acid (PLA) material was printed over the top of an Acrylonitrile-Butadiene-Styrene (ABS) printed workpiece; however, the bond strength between new and existing material in this re-printing process was not analyzed, which could have provided some insight on improving the mechanical properties of the parts.

Another goal in AM research is to print on injection-molded enclosures that are embedded with active components. With the development of low-cost 3D printers, the approach to fabrication has changed drastically. Objects are customized, designed and fabricated by individuals according to their personal needs. Designers are thinking creatively to fabricate high-tech products with higher complexity. There is a growing interest in incorporating functional elements such as sensors and chips into 3D printed parts. Gao, Zhang, Nazzetta, Ramani, & Cipra (2015) built a multi-directional printer called "Revomaker" to print fully functional devices such as computer mice and toys. Revomaker has a cuboidal base, which may be rotated about all three axes for printing. This feature reduced the material used for support as well as printing time. Functional modules were pre-assembled inside a cuboid, which was manufactured by an injection or blow molding process. The cuboid was closed and part geometries were printed on top of the cuboid. Multi-directional printing reduces material consumption and enables printing products with embedded functionality (Gao *et al*., 2015). Printing on top of existing parts created by traditional polymer manufacturing processes can significantly reduce printing time. This allows integration of traditional manufacturing processes such as machining, milling, and/or injection molding with AM to build complex geometries without the need for assembly.

The works discussed thus far have focused on reducing the printing time, material consumption, surface roughness, and anisotropies in the workpieces of AM processes. In all cases, a new layer was deposited on top of an existing workpiece or substrate. This leads to a critical need to understand how process parameters affect bond strength between the first layer and substrate, and by extension, the mechanical strength of the final part.

None of the above discussed methods have directed their attention towards bond strength when depositing a new layer on an existing surface. This becomes important because the strength of this bond determines the strength and integrity of the final part. From the adhesion theory it is known that surface roughness plays a significant role in adhesive bonding (Budhe, Ghumatkar, Birajdar, & Banea, 2015). However, this has not been verified in the case of AM. Verifying this will help manufactures to integrate subtractive and AM process together to reduce printing time and also improve strength. To achieve this, it is important to know how the surface condition of a previously manufactured part affects the bonding process. If it does, it is necessary to identify the best process parameters that can used to achieve good bond strength between existing surface and new layer deposited. This also helps in developing a hybrid process for patching/re-manufacturing and 5/6 axis printers, where process parameters can be altered in the middle of the printing process to achieve significant bond strength in different directions.

2. Problem Statement

The objective of this research is to investigate the effect of substrate surface condition and AM process parameters selected for an auxiliary part on the bond strength between the substrate and auxiliary part. The relationship between the AM process parameters and mechanical strength (and by extension the adhesion between consecutive layers) has been well examined in the literature (Fatimatuzahraa, Farahaina & Yusoff, 2011; Sood *et al*., 2009; Oropallo *et al*., 2016; Christiyan, Chandrasekhar, & Venkateswarlu , 2016; Sun, Rizvi, Bellehumeur, & Gu, 2008; Li,Sun, Bellehumeur, & Gu, 2002). The general trends may likely be extended to printing on a substrate of the same material. It is also likely that the surface condition of a previously manufactured substrate significantly affects the adhesion strength. However, there is very little evidence in the literature to support or refute this assumption. The selection of process parameters used to manufacture the auxiliary part and the most relevant surface roughness metrics of already manufactured substrate must be identified in order to facilitate effective process control in patching/re-manufacturing processes. This, in turn, will facilitate production of functional, customized components with maximum strength.

This work tests the hypothesis that for printing atop previously a manufactured substrate, bond strength is a function of substrate surface condition, layer thickness, and raster angle at which the auxiliary part is printed. If the hypothesis tests true, then, factors which include surface roughness of the substrate, raster angle, and layer thickness of the auxiliary part that significantly affect the bond strength, will be screened. In addition, regression analysis will be used to develop a prediction model as a function of surface roughness, layer thickness and bond strength. Should the hypothesis test false, it is intended to add additional AM process parameters to check if adding new parameters to the existing ones show any effect on bonding.

3. Literature Review

A literature survey was conducted to study the previous work in the field of layer-to-layer bonding, the influence of surface condition on adhesion, and the process parameters affecting the roughness of a 3D printed part.

3.1 Layer-to-Layer Bonding

The current literature on layer-to-layer bonding focuses on the bonding phenomena for building print all at once. Since the bonding process in AM is driven by heat, it is expected that the theory of layer-by-layer bonding also applies in the case of printing on top of an existing substrate fabricated via any manufacturing process.

To achieve a quality bond between the substrate and an auxiliary part it is necessary to understand the bond formation dynamics in AM. Adhesion between layers depends on the amount of thermal energy the material holds when it is extruded. Build plate and extruder temperatures play a crucial role in building a good, quality bond between layers of the printed part (Sun *et al*., 2008). The process of bonding in FFF involves wetting, i.e., molten material deposited from the extruder maintains contact with the existing layer. Wetting of a surface leads to neck formation between the filaments. Furthermore, diffusion of molecules and randomization occurs across the interface **(**Li *et al*., 2002). Strength of the bond is dependent on neck formation (see Figure 3.1) between the beads of molten polymer as a result of wetting and molecular diffusion at the interface. This process is called sintering (Gurrala & Regalla, 2012). The quality of the bond formed is dependent upon the neck formed between filaments. Turner, Strong & Gold (2014) proposed that bond strength between two adjacent molten filaments beads depend on the contact area between the beads and is influenced by the width of the filament deposited. Strength of a 3D printed part is limited by the bond strength between the neighboring beads of polymer (Gurrala *et al.*, 2012). Bond strength is also dependent on the contact area between the beads and is a function of the energy of cohesion/adhesion. Good bond strength between the layers deposited can be achieved by printing above the glass transition temperature of amorphous polymers. (Turner *et al.*, 2014)

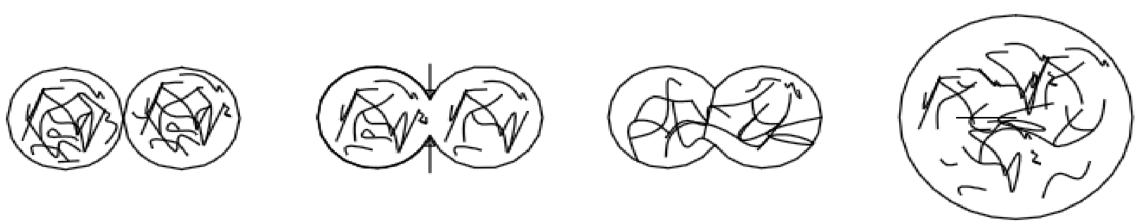

Figure 3.1. Sintering process between two laid filaments a) Surface contacting b) Wetting c) Diffusion d) Randomization (Li et al., 2002)

Hence, it is understood that the bonding phenomena in AM process is dependent upon extruder and bed temperatures. Increasing the temperature or adding heat to the substrate would improve the adhesion of the first layer. Sun *et al*. (2008), in their paper conducted heat transfer analysis of an FFF process to evaluate bond formation dynamics between filaments. They found that bed temperature and changes in convective conditions inside the heat chamber had a strong influence on the mesostructures and bond strength quality between the filaments. Controlling the cooling conditions inside the chamber had greatly impacted the accuracy and mechanical properties of the fabricated parts.

Along with temperature analysis, there is a need to analyze the effect of process parameters on bonding phenomena. Pan, Huang, Guo & Liu (2016) studied the effects of slice thickness and nozzle translation velocity on the adhesive strength of PLA. They varied the slice thickness, nozzle velocity, and fill rate by conducting orthogonal experiments. It was found from their results that the adhesive strength between layers increased with an increase in the nozzle velocity and slice thickness to a point; however, the strength declined with additional increase in these parameters. Slicing thickness has a significant influence on adhesive strength when compared to nozzle moving rate due to thicker layers and concomitant heat accumulation.

In conclusion, AM process parameters (especially temperature) play a crucial role in bond formation between molten filaments; however, the influence of surface roughness has not been addressed yet. Coarser surface roughness could affect the bond strength either positively or negatively by altering the contact area with the molten material and the base part. High surface roughness might impede the flow of molten material into valleys, as shown in Figure 3.2, thereby reducing the contact area between the substrate surface and molten material. The ability of material to flow into the valleys reduces if its viscosity increases, *viz.* it sits on top of the peaks reducing the contact area between surfaces as shown in Figure 3.2. Alternately, if the melt does fill the valleys, surface roughness might increase contact area and improve the bond strength.

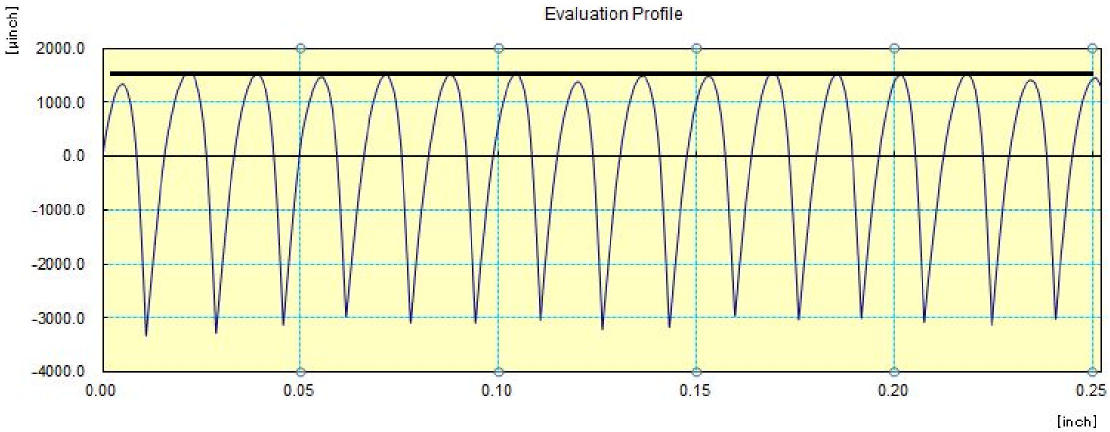

Figure 3.2. New layer deposited on the surface profile of existing part

3.2 Influence of surface condition on adhesion

Wetting is considered to be an important phenomenon, which determines the quality of a bond between the adhesive and its adherent. Brockman, Geiß, Klingen, Schröder, & Mikhail (2009) discussed the wetting principle in adhesive bonding. Wetting can be observed when a liquid drop spreads over the surface of a solid material. Depending on the condition of surface, a liquid drop forms a contact angle between its surface and the surface of solid material. This angle ranges from 0° to 180°. At 0°, the liquid spreads over the entire solid surface and wets it completely, while at 180° no wetting happens. The condition of the surface determines the contact angle of the molten material in re-printing processes. Wegman, & Twisk (2012) also propose that surface roughness is considered to be a contributing factor in adhesion theory. For effective bonding between the substrate and its part, adhesive must wet both the surfaces. Therefore, it is necessary to consider the surface roughness condition of the substrate to understand bonding phenomena. Hence, in 3D printing, strong bonding between the substrate and an auxiliary part can be achieved if the molten material deposited by extruder wets the surface completely.

In order to understand the flow of molten material on the surface, it is necessary to know the roughness profile of a surface. Valleys, peaks, and spacing surface roughness parameters help in understanding the contact area developed between the substrate and the molten filament. Parts fabricated through manufacturing techniques such as machining, injection molding, and AM have a particular texture and roughness on their surface. Quantifying the surface into amplitude and spacing parameters helps in measuring the inhomogeneity of the surface and distance between its surface anomalies (Cubberly & Bakerjian, 1989). Amplitude parameters, depicted in Figure 3.3, include R_a (arithmetic mean deviation), R_{sk} (skewness), R_p (max profile peak height), and R_z (average peak to valley height), while spacing parameters are R_{pc} (peak count) and S_m (mean spacing) (Udroiu & Mihail, 2009). Measuring the depth of the valley between two adjacent peaks can help to understand the penetration power of the molten material into the valley.

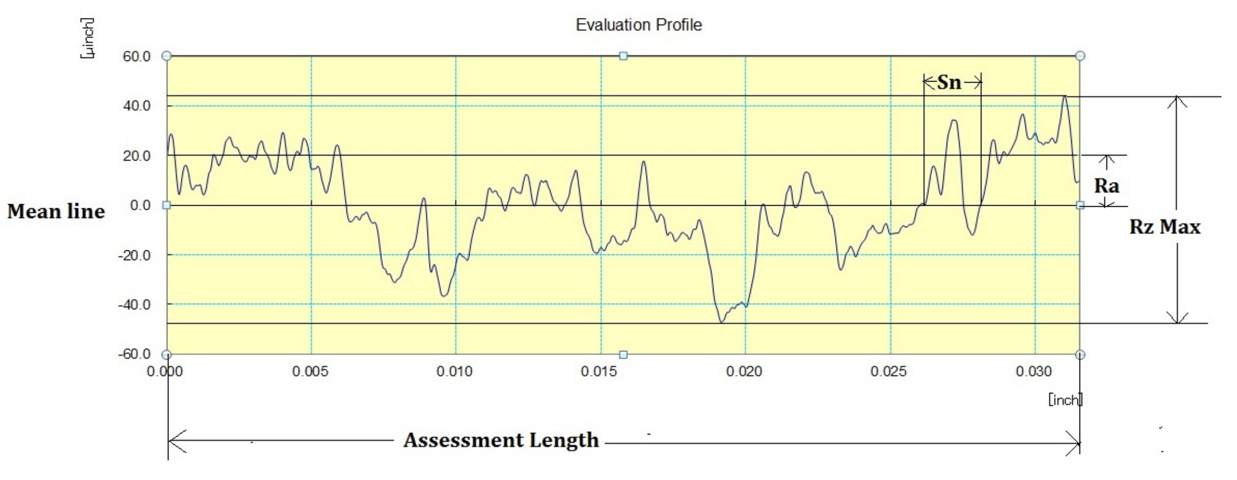

Figure 3.3. Surface roughness amplitude parameters

The surface condition of a part can also be characterized by the directionality or pattern of the surface roughness. Varying direction of irregularity is exhibited in many surfaces manufactured through different processes. The direction in which these irregularities predominantly exist can be defined as surface lay. Lay provides information on the deposition angle to be considered for effective flow of molten material into voids. Krolczyk, Raos, & Legutko (2014) investigated the surface integrity of parts fabricated through both turning and FFF processes. It was found that an anisotropic and periodic structure was found on the surface by turning process. The surface obtained by FFF technology was composed of high peaks when compared to machined surface. Also, large fluctuation was observed in roughness parameters for a printed sample. The surface obtained after turning was smoother than the surface obtained using FFF technology. According to surface profile analysis for FFF samples, the surface roughness of FFF parts is relatively high compared to subtractive manufacturing processes indicating that the valleys and peaks on machined surfaces are smaller compared to parts printed using AM.

3.3 Process parameters affecting the surface roughness

AM process parameters play a key role in determining the accuracy and surface quality of 3D printed parts. Parts tend to have rough surface finish due to a staircase effect caused by layered deposition. It is important to decide on the process parameters that must be varied for printing substrates as the chosen parameters determine the roughness of substrates.

Anitha, Arunachalam & Radhakrishnan (2001) assessed the influence of process parameters on the quality of AM prototypes. They considered layer thickness, road width, and speed of deposition as factors in their experiment. Road width is the thickness of the bead of material the nozzle deposits. It was observed that the layer thickness had a significant effect on roughness under interacting and non-interacting conditions. At a 99% confidence interval, the layer thickness was 51.57 % significant, while the speed and road width contributed 15.82 % and 15.57 %, respectively. It was concluded through correlation analysis that the layer thickness is inversely related to the surface roughness.

Sreedhar, Manikandam & Jyothi (2012) studied the effect of angular orientation on the quality of parts built with inclined surfaces. Parts built with inclined or curved surfaces have higher surface roughness due to the stair stepping effect. A profilometer was used to calculate the surface roughness values along the inclined surface. Improved surface roughness was achieved when the part was printed at 20^0-30^0 degrees to the build platform. The build orientation had a significant impact on the surface roughness of the FFF printed parts.

Vasudevarao, Natarajan, Henderson, & Razdan (2000) proposed that choosing optimal process parameters can aid in achieving best surface finish for the parts. Their fractional factorial design was conducted considering build orientation, layer thickness, model temperature, air gap (space between the beads of deposited material), and road width as five factors. ANOVA results suggested that the layer thickness, build orientation, and their interaction had a significant effect on the surface roughness of the parts. P values were 23.8828 %, 41.51 % and 18.40 %, respectively.

The other contributing factor for roughness on 3D printed surface is the development of voids between the layers deposited. Using low layer thicknesses would reduce the surface roughness by reducing the cusp height between the layers. However, this would increase the build time and cost of printing (Alhubail, 2012).

From the literature, it is concluded that layer thickness and build orientation have significant effect on the surface finish of AM parts. Concerning the challenges in AM, the stair stepping effect and anisotropic properties are believed to be major problems affecting the accuracy and strength of parts. Varying layer thickness and build orientation can reduce these problems to some extent. As per literature, varying the layer thickness, and build orientation can help achieve different roughness values on the substrate surface.

4. Methods & Experiments

This section describes the tools, materials, testing equipment, experimental procedures, and analysis methods used throughout this research.

4.1 Full factorial analysis

A full-factorial, two-level design of experiments was conducted to study the joint effect of three factors on the response. The objective was to screen the significant factors and their interactions for further analysis. The factors and levels listed in Table 4.1 were selected to understand their influence on bond strength. Each condition was replicated five times. More than one replicate was used because a single run of the experiment may not give accurate information about the effect of all the factors on bond strength. Also, for a screening experiment, having many replicates is not feasible. Hence, considering the time and resources available for research such as printing material, heat chamber, and importantly, the printer, the number of replications was limited to five. Layer thickness, raster angle, and surface roughness were considered as the factors and the bond strength was the response.

Table 4.1. Factors and levels considered for experimentation

Factors	Low Level	High Level
Layer thickness	0.180 mm	0.30 mm
Raster angle	0°	90°
Surface Condition	Substrates fabricated through extrusion process with lower roughness level	Substrates fabricated through AM process with higher roughness

The bond formation process is dependent on temperature, and it was hypothesized that bond strength would improve with increase in layer thickness because higher deposition rate would increase the amount of heat flow into the fusion zone. Additionally, higher layer thickness increases the amount of molten material available to flow into the valleys of the surface profile. Considering the amount of heat and material flow into the fusion zone for significant bond formation, levels of 0.18 mm and 0.30 mm were considered for layer thickness.

Raster angle in this research is the angle at which molten bead is deposited relative to the lay of substrate. It is hypothesized that raster angle may affect the molten material's ability to flow into the valleys of the surface profile. Also from the literature (Sood, Ohdar, & Mahapatra, 2012), the direction in which tool deposits the molten material on the substrate affects the strength as the raster angle either decreases or increases the length of rasters deposited. The two levels selected for raster angle was 0° and 90°.

The amount of molten material that flows into the valleys on a surface was expected to influence the strength of bond. Hence, surface roughness was considered as another factor. It was important to select the roughness parameters to get better insight into molten material flow on the surface of substrate. Hence, roughness average (R_a) and mean spacing (R_{sm}) were analyzed as amplitude and spacing parameters. The R_a value was 10.7µin and 1034µin for extruded substrate and AM substrate respectively. Higher surface on AM substrate was due to severe stair stepping; on the other hand R_{sm} value was 16650.8µin and 11475µin for AM and extruded substrates .The bond formed in this experiment was evaluated using tensile testing process and the maximum load that the bond can withstand before it breaks was recorded.

4.2 Regression analysis

Screening experiments helped identify the factors that significantly affected the bond strength in a patching/remanufacturing process. If the process parameters and surface roughness have an effect on response, it is necessary to quantify them to print parts with better mechanical strength. Regression analysis is used in this research to develop a model for estimating the relationship between layer thickness, surface roughness and bond strength. It was found from full factorial experiments that layer thickness and surface roughness have significant effect on bond strength. Hence, these two factors were retained and the raster angle was dropped for further analysis. As it is not possible to estimate the quadratic effects with a two level design, an additional level was included for each of these factors to detect said quadratic effects, if any. A layer thickness of 0.24mm was added as another level lying between 0.18mm and 0.30mm layers and a new surface roughness level of 765µin was added between the two used in the prior experiment i.e., 10.7µin (extruded) and 1034µin (AM fabricated at 45° to x-axis).The factors and levels considered for regression analysis are given in the Table 4.2.

Table 4.2. Experimental factors and levels for regression analysis

Factors	Level-1	Level-2	Level-3
Layer thickness	0.18 mm	0.24 mm	0.30 mm
Surface condition	Substrates fabricated through extrusion process with lower roughness level(R_a-10.7 µin)	Substrates fabricated through AM process in Z-direction (R_a-765 µin)	Substrates fabricated through AM process with higher roughness (R_a-1034µin)

Considering the time and cost to run experiments for additional level of factors, five replications were run for each condition to verify the variability in design. After discovering the significant terms in ANOVA table, insignificant terms were dropped from the model. Finally, a prediction model was developed. Microsoft excel solver was used to find the optimal values for surface roughness and layer thickness.

4.3 Specimen Design

Autodesk Inventor software was used to design the specimens. The specimen is built in two parts: substrate and auxiliary part. Two types of substrates, as shown in Figure 4.1 were designed in two colors, i.e., black and white. The auxiliary part was fabricated in red and was printed on the top of substrates. The motivation for using different colors for the parts was to have a clear visual understanding of the fracture interface after bond failure.

AM substrates were designed as rectangular blocks of size 48 x 30 x 17 mm. The black substrate was machined from extruded ABS bar stock, and the white substrate was fabricated via FFF. The black substrate, as pictured in the Figure 4.1, was the lowest surface roughness level and the white substrate had the two higher surface roughness values. The 3-view drawing can be found in Appendix A.

Figure 4.1. Substrates

An auxiliary part, as shown in Figure 4.2, was designed initially to evaluate the bond strength. The test section was 90 mm in height and 20 mm in diameter (cylindrical cross section over the gage length). The 3-view drawing of the auxiliary part can be found in Appendix A. Results from tensile test indicated that repeatability was very poor with this design. Moreover, many specimens failed at the intersection of shoulder and shaft as pictured in Figure 4.3. The reason for this failure can be attributed to the stress concentration, voids, or holes created in the part during fabrication with AM. Also, the time required to print these specimens was considerably high. Hence, this design was modified to reduce printing time, material consumption, and variability in data.

Figure 4.2. Auxiliary part

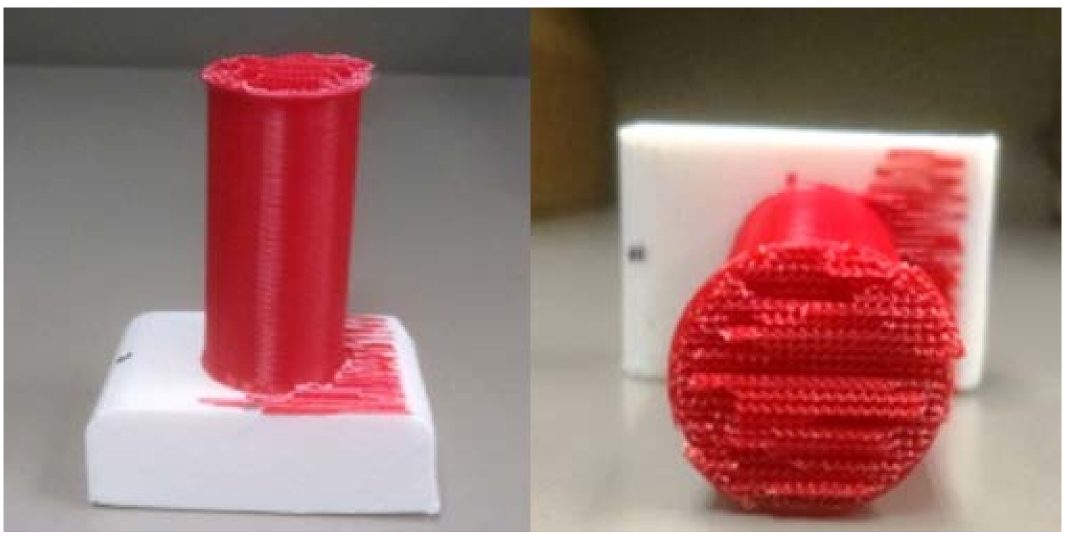

Figure 4.3. Area of failure at intersection of shoulder and shaft

The gage portion was changed from cylindrical cross section to a tapered design as shown in Figure 4.4. The square cross section at the bottom increased the area of contact between the substrate and auxiliary part. The sharp corners along the shoulders were filleted to avoid stress concentrations. The length of the sample was shortened by 10 mm to reduce the time to print. All the data reported during the course of this research were obtained using this design. Most of the samples broke at the bond. Those that failed elsewhere were discarded and new samples were printed to obtain data. It was found that the variation in the data was far less when compared to those for earlier design.

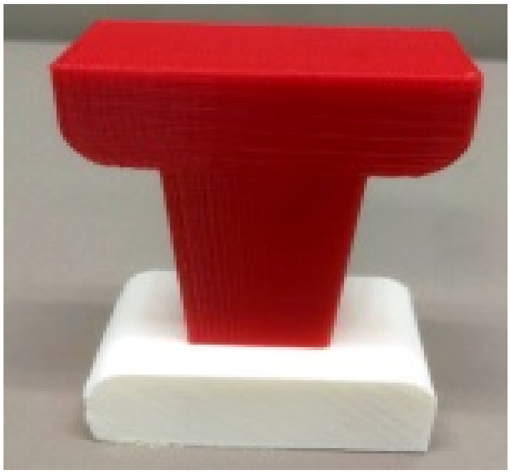

Figure 4.4. Modified auxiliary part

4.4 Tests and measurements

Since surface roughness is an important factor, surface profile measurements were carried out using a SURFTEST SJ 210 made by Mitutoyo. A vertical stylus was affixed to the device and the displacement of this stylus along the part surface was processed based on which the roughness profile was displayed on the screen. The maximum range of this SURFTEST SJ210 was 360µm (-200 µm to +160 µm).

The procedure followed for obtaining the surface roughness values complied with standard ANSI B46.1 for amplitude and spacing parameters. The surface roughness of all the substrates was accessed along the long dimension, as shown in Figure 4.5. The samples were assessed at a stylus speed of 0.400 mm/sec at an evaluation length of 0.157 in. The surface roughness of all the 40 samples was measured three times for all amplitude parameters. The details of surface roughness values obtained through surface analysis are discussed in Appendix B.

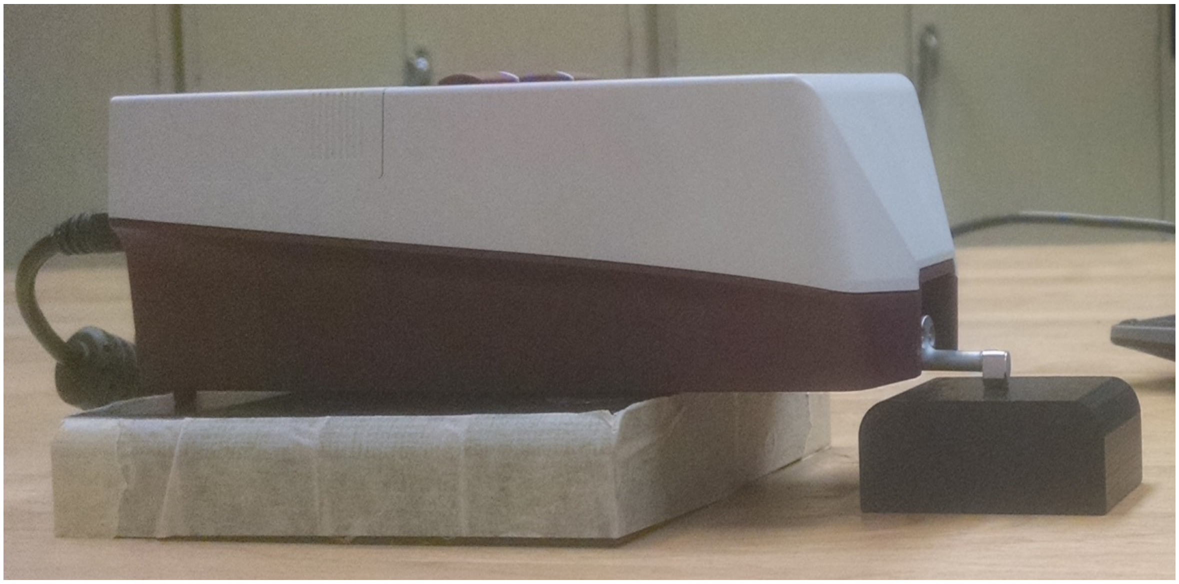

Figure 4.5. Surface profile analysis

Tensile testing was used in this research to measure the bond strength. Tests were carried on MTS micro console tensile testing machine with a load cell of 20 kips as shown in Figure 4.6. The ASTM D 638 standard was followed to perform tensile tests on the specimens. The specimen for the test was placed in the grips and sufficient clearance was provided to avoid loading the specimen before starting the test. The speed of crosshead throughout the testing process was set to 0.04 in/min. Load vs elongation data was automatically recorded by the tensile testing machine's software. Load was measured in pounds and elongation was measured in inches.

Engineering stress was chosen to quantify bond strength, and is given by

$$S=F/A_o$$

where, S is Engineering Stress (lb/in^2), F is applied tensile force (lb), and A_o is the original area of the test specimen (in^2) taken prior to loading (Groover, 2012). Area of all specimens at the bond interface was 0.62 in^2. Figure 4.7 shows the interface of the substrate and auxiliary part after bond failure.

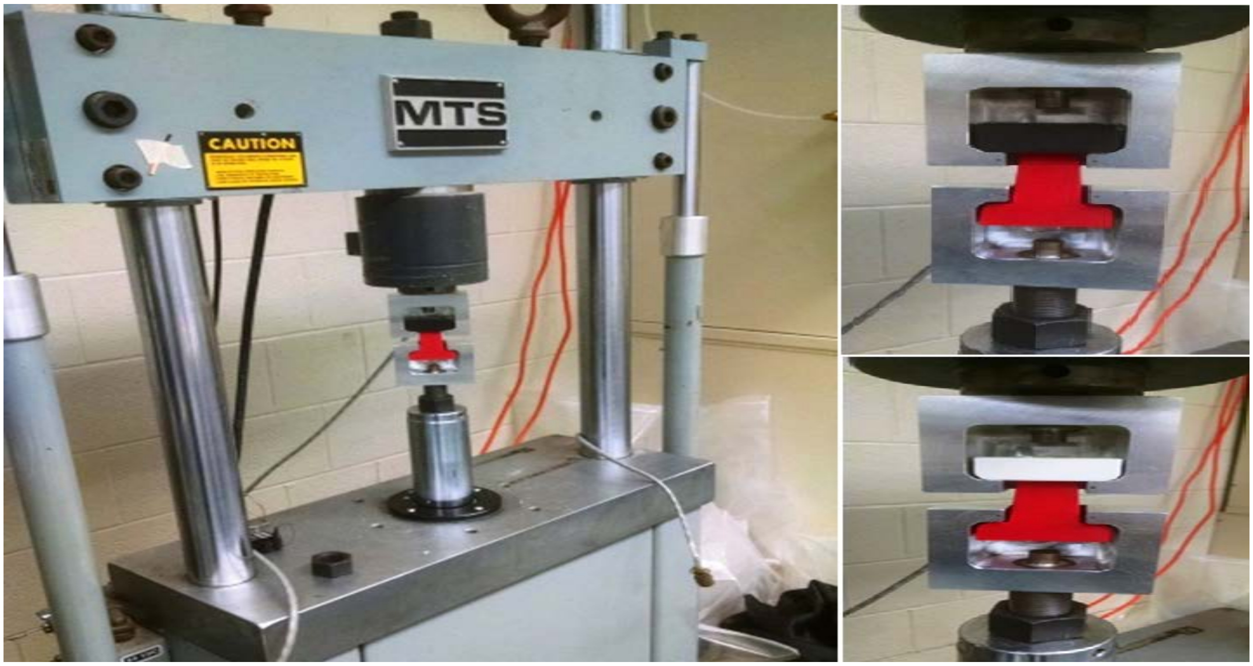

Figure 4.6. Bond strength testing on micro console tensile testing machine

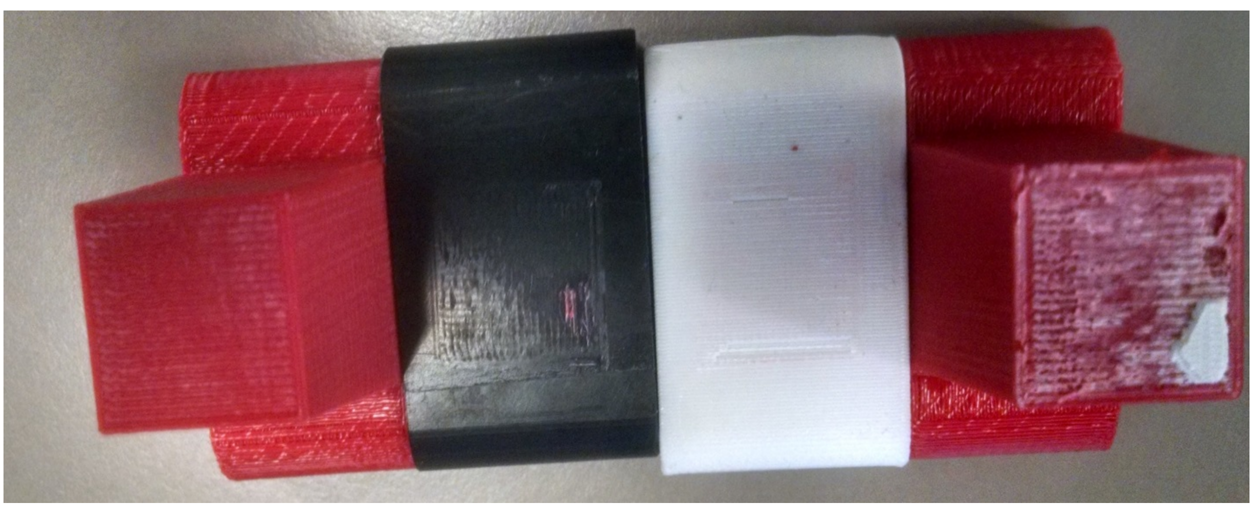

Figure 4.7. Interface of the substrate and auxiliary part after tensile testing

Aluminum grips were machined to hold the specimen in the tensile testing machine. These are shown in Figure 4.8 and were designed to hold the specimen without clamping or applying transverse strain. The 3-view drawing of grips can be found in Appendix-C.

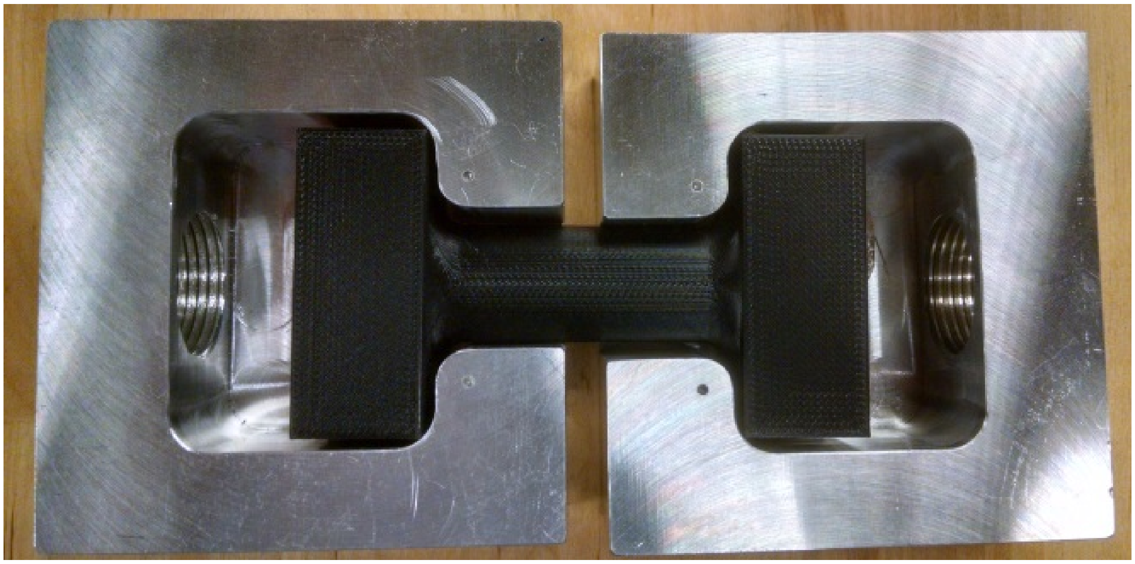

Figure 4.8. Grips for tensile testing

4.5 Substrate and auxiliary part fabrication

AM substrates were fabricated from ABS polymer on a maker gear M2 printer. The substrates were printed at an angle of 45° relative to the x axis of the printer as shown in the Figure 4.9. The basis for printing at an angle of 45° was to maximize surface roughness due to stair stepping. The middle-level roughness substrates, used for additional full factorial experiments, were printed at an angle of 90 ° relative to the build plate. Process parameters used to print substrates are listed in Table 4.3. The lowest surface roughness substrate was machined from rectangular ABS bar stock.

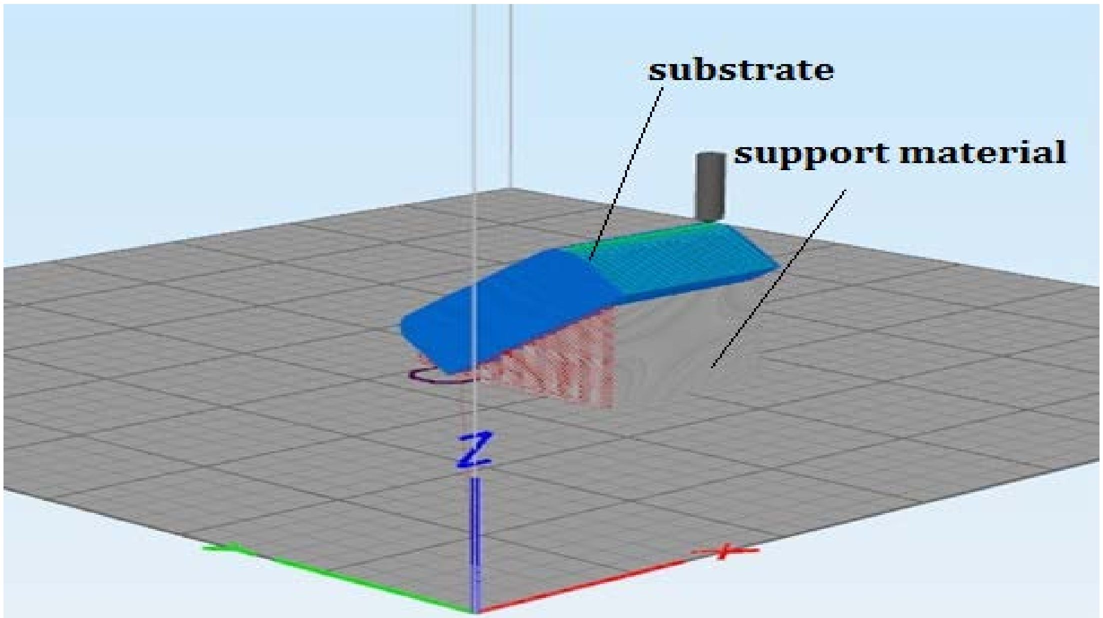

Figure 4.9. Substrate fabrication 45° relative to X axis

Table 4.3. Process parameters used to fabricate substrates

	Process parameters for substrates (10 specimens)	
Surface Condition-1	Build orientation at 45° to the build plate (AM process)	
	Nozzle diameter	0.36 mm
	Primary Layer thickness	0.3
	Substrate filament color	White
	First layer speed	15 % of 3600= 540 mm/min
	Raster angle	45,-45
	Infill percentage	60%
	Extruder temperature	235 °C
	Solid Infill under-speed	80 % of 3600= 2880 mm/min
	Filament diameter	1.75 mm
	Chamber temperature	36 ± 2 °C
Surface Condition-2	Un-machined surface	Extrusion process

The AM parts were initially printed at room temperature, but the ABS material exhibited shrinking and curling. This could influence the bond formed between the substrate and the auxiliary part. To avoid warping, a heat chamber was designed and a PID controller was set up to control and maintain constant and slightly elevated temperature. An electrically heated plate was placed inside the heat chamber and the set point of the PID controller was 36°C. Two fans were connected to the PID controller to help with heat distribution and exhaust. One fan aids in maintaining uniform temperature by circulating hot air in the chamber, and the exhaust fan helps in venting and cooling if the temperature increases beyond the desired value. Temperature was recorded for all the samples through data logging software (Cool Temp) and the printing temperature for all the specimens was maintained between 36-38°C.

The AM substrates that were printed at an angle of 45° relative to the X-axis exhibited significant unevenness on their bottom surface. This led to unevenness in the substrate orientation upon affixing it to the build plate as seen in Figure 4.10. Hence, the bottom portion of the AM substrate was machined to ensure that the top surface was as level as possible before the auxiliary part was printed on the top. A dial indicator was used to measure the unevenness of the substrate surface after fixing it on the build plate. Final leveling, if needed, was accomplished by placing double=sided tape placed under one end of the part.

Figure 4.10. Unevenness when substrate is printed at 45 ° relative to the X-axis

Printing the auxiliary part on the top of substrates required modifying the tool path of the extruder. Hence, measuring the height of the substrate accurately became extremely important to obtain consistent results. Digital calipers were used for measuring the height of the substrates. Five readings in different directions were taken and the mean of all the readings was calculated to mitigate the effect of any deviation in the measurement. Unlike a typical printing process, this experiment aimed to deposit molten material on the top of an existing part which required coding a tool path from a pre-determined height. Marks on the surface of the build plate aided in locating the substrate consistently. Since the height of substrate was known, the machine code for the auxiliary part was adjusted to ensure printing occurred exactly on top of the substrate. Hence, the first layer of printing started from the 50-56th layer in the G-code which depended on the dimensions of the substrate as shown in Figure 4.11.

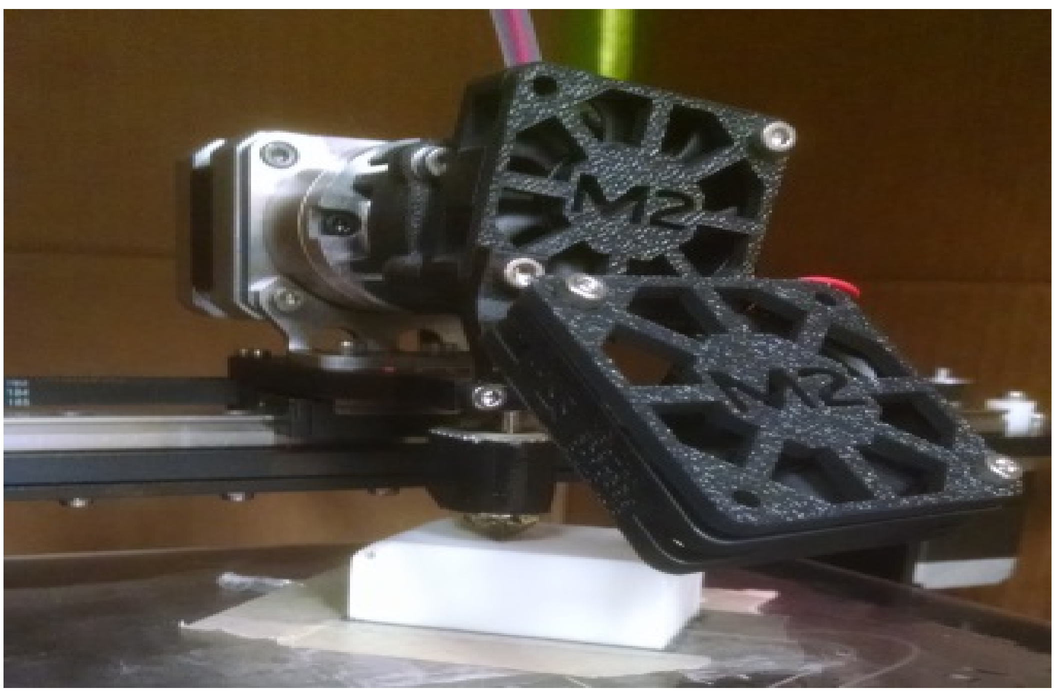

Figure 4.11. Modified G-code to printing on the top of substrate

Any movement of the substrate during the printing process affected the bond formation. To avoid this issue, substrates were glued to the glass plate using super glue. The slicing and toolpath software, Simplify 3D, was limited to a few pre-defined infill angles. The substrate was rotated on the build plate in order to print the 0° and 90° raster angles relative to the substrate surface lay, as shown in Figure 4.12.

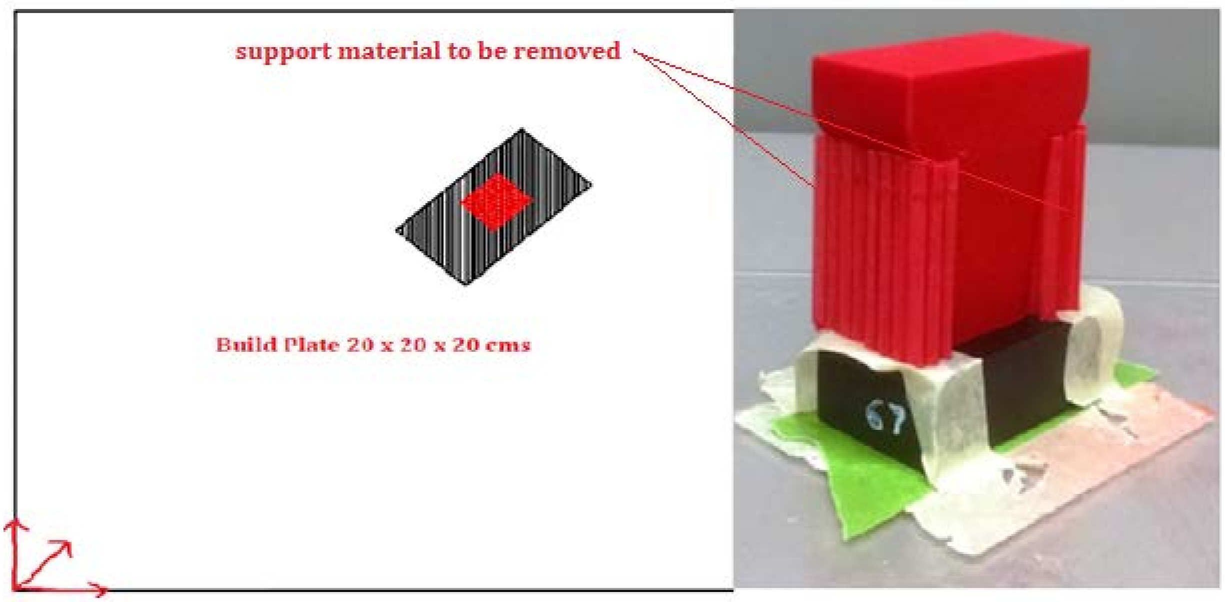

Figure 4.12. Substrate orientations for printing at different raster angles

It was discovered early on that the bond strength was highly dependent on the z-position of the extruder. Nominally, the extruder would start printing the first layer of the auxiliary part at a height relative to the top of the substrate equal to the layer thickness. This practice was found to produce very weak bonds, so a distinct 1st layer height parameter was included. 1st layer height is defined as zero when the extruder just touches the top of the surface profile of the substrate, and a negative value indicates the tip of the extruder is actually penetrating into surface of the substrate. This is illustrated in Figure 4.13. A 1st layer height of -0.27 mm was used in fabricating all samples for the full-factorial experiment and the regression analysis experiments.

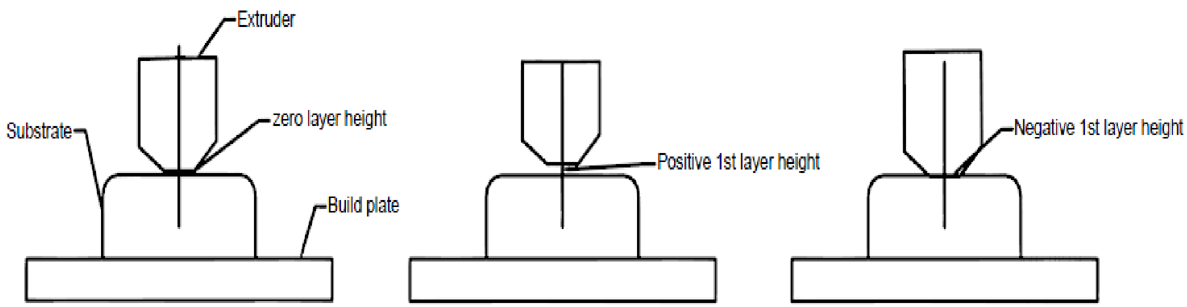

Figure 4.13. Extruder and substrate contact height

5. Results & Discussion

5.1 1st layer contact height between nozzle and substrate surface

As discussed in the preceding section, 1st layer height was important for bond formation. This height is generally positive for FFF process, i.e., the extruder does not have any physical contact with the build plate surface. A minimum gap between the extruder and the build plate allows molten material to be deposited and bonded to the build surface. This principle was applied in the experiments initially and the 1st layer height between the extruder and the substrate was maintained positive for one cycle of experiments. The bond formed using this condition was weak and it failed while removing the part from the build plate. However, under other conditions, the bond was slightly stronger and failed at up to 81psi stress. All the samples printed with the aforementioned condition failed in this range. Specifically, AM substrates were slightly stronger than the extruded substrates and therefore lasted until the tensile testing stage. Since bond formation between the substrate and auxiliary part was vital to test the research hypothesis, some modifications were performed with respect to the 1st layer height to improve the bond formation process. Response values for 40 experimental runs were obtained by maintaining a negative 1st layer height as shown in Figure 4.13. Negative 1st layer height allows the hot extruder to touch the surface of the substrate, thereby melting the top surface in the immediate vicinity of the extruder. This sintering between the substrate and the new molten bead that is deposited from the extruder helps in forming a bond. The bond formed with negative 1st layer height was found to be significantly stronger in comparison to the bond formed with a zero 1st layer height. Figure 5.1 shows a graphical analysis of the difference in the bond strengths used in these methods.

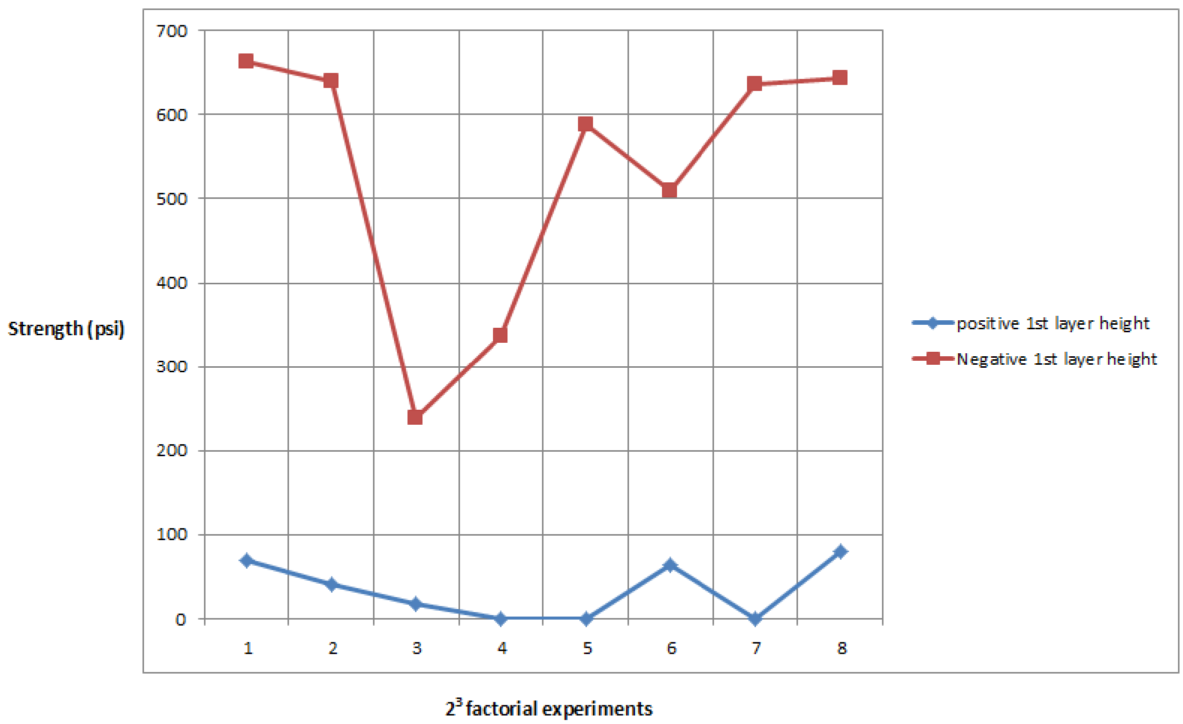

Figure 5.1. Variation in the samples printed with different 1st layer heights

A set of experiments were conducted to more carefully examine the effect of 1st layer height. The height was varied from 0 to -0.27 mm. A height of -0.27 mm was chosen as exceeding this level was found to seal the gap between the extruder and the substrate causing restriction of the flow of molten material from the extruder. The AM process parameters, surface roughness selected, and bond strength values obtained in this experiment are listed in Appendix D. A regression analysis was performed, as shown in Figure 5.2, to predict the influence of 1st layer height on strength. The relationship was found to be

$$\sigma = 7.82 - 1767\,x$$

where σ is bond strength and x is the 1st layer height . An R^2 value of 69.9 % indicated a minimum variation in the data for an increment in the 1st layer height. The analysis shows that making the 1st layer height more negative improves the bond strength between the substrate and the auxiliary part.

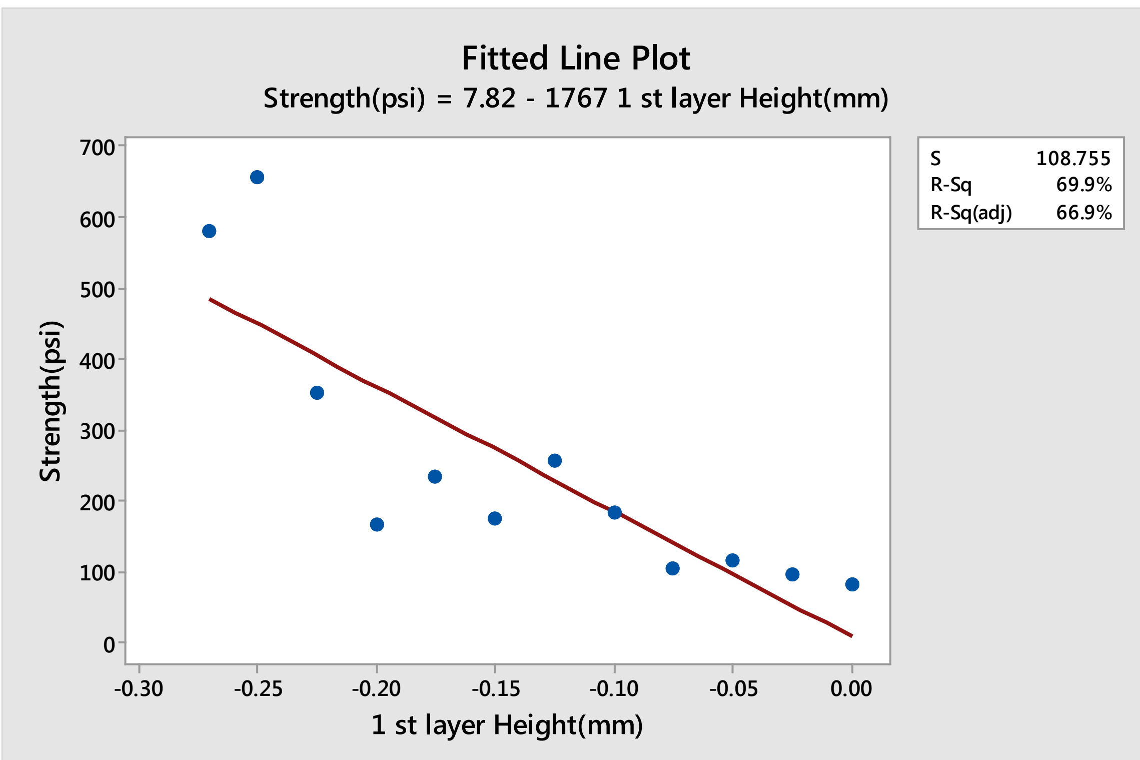

Figure 5.2. Fitted line plot for various 1st layer heights

5.2 Full factorial analysis results and distribution plots

A full factorial analysis was carried with five replications of each condition and the design matrix for analysis is described in Appendix E. Conducting full factorial design analysis allowed estimating the mean, which further provided information on the impact of each factor on the response characteristic. Analysis of variance (ANOVA) was used to conduct statistical inferences on the equality of means based on the factors that showed a significant effect on the response. The total strength values associated with each run of 8 experiments and 5 replicates are listed in Table 5.1. This data helped to provide insight into the factors affecting the bond strength. It was observed from the data that bond strength values appeared to be higher in some of the experimental runs, while lower in others. This result indicated that bond strength was affected by the selected factors. Variance present between replicates for a few conditions were found to be considerably large. This may be due to blocking or nuisance factors in the experiment such as chamber temperature, and slight deviations in substrate dimension that were caused due to irregularities in the bottom of the substrate. However, these were identified prior to start of the experiment and every effort was taken to maintain them as close to constant as possible. The effect of blocking factors on response was minimized but couldn't be eliminated. Parametric tests like ANOVA, Regression, and DOE work robustly on the normality assumption. Considering the variation in the data, and the robustness of the aforementioned tests to normality assumptions there was a need to check for normality in data obtained. Since the data was continuous and the sample size being 40, some of the assumptions for normality hold. Further, Anderson Darling test was performed to verify the normality in data. The results of the test are shown in Appendix F. A confidence level of 95% was considered and compared with the p-value from the normality test. This test suggested that the residuals followed a normal distribution.

Table 5.1. Results from experimental runs

Coded factors			**Bond strength (replicates)**					
A	B	C	R1(psi)	R2(psi)	R3(psi)	R4(psi)	R5(psi)	Total
-1	-1	-1	289.06	635.58	403.25	548.95	749.77	2626.62
1	-1	-1	309.677	777.33	643.45	541.08	367.822	2639.37
-1	1	-1	127.62	237.96	182.74	186.67	119.74	854.75
1	1	-1	245.74	261.5	336.3	119.82	159.11	1122.48
-1	-1	1	411.12	588.32	529.25	513.51	324.5	2366.72
1	-1	1	434.75	387.5	379.62	332.37	509.58	2043.83
-1	1	1	615.88	218.17	663.14	189.88	505.64	2492.74
1	1	1	277.24	293	537.14	548.95	639.51	2295.85

Probability distributions (Figures 5.3, 5.4, & 5.5) were plotted for various conditions to check differences in the mean and variances. The variation in the extruded surface condition was greater in comparison to the AM surface conditions. Possible reasons for variation in the data could be as follows:

- Dimensional issues due to irregularity at the bottom surface of the substrate.
- Warping effect due to rapid cooling of ABS material.
- Minute unevenness in the build plate of the machine.
- Temperature in the heat chamber.

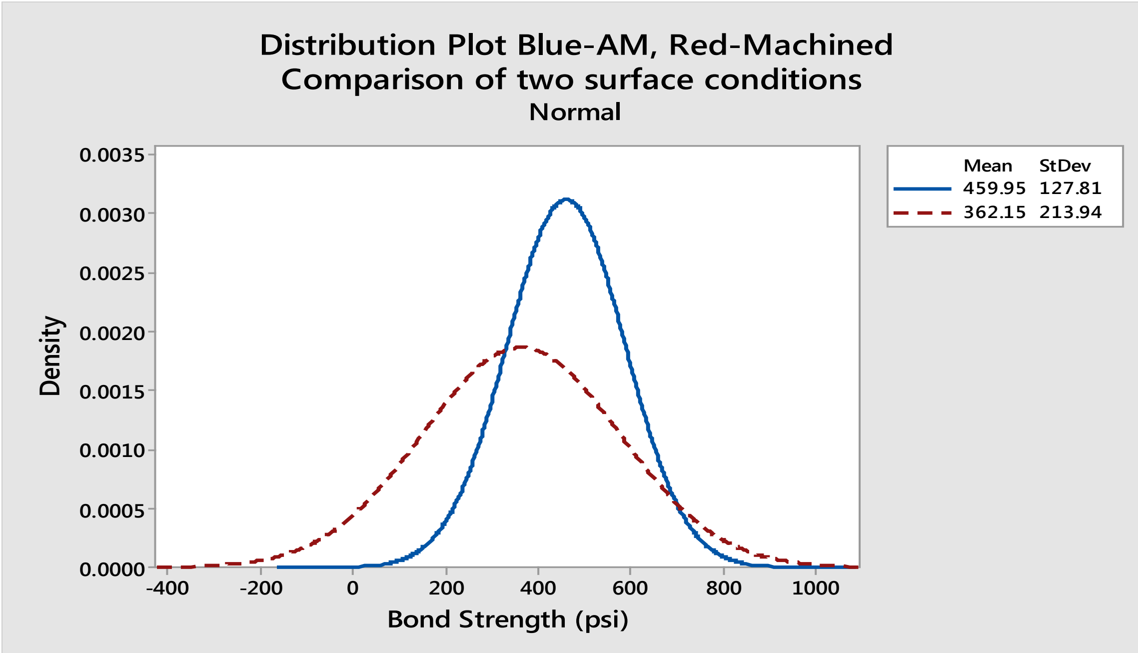

Figure 5.3. Distribution plot for mean strengths of AM and machined substrates

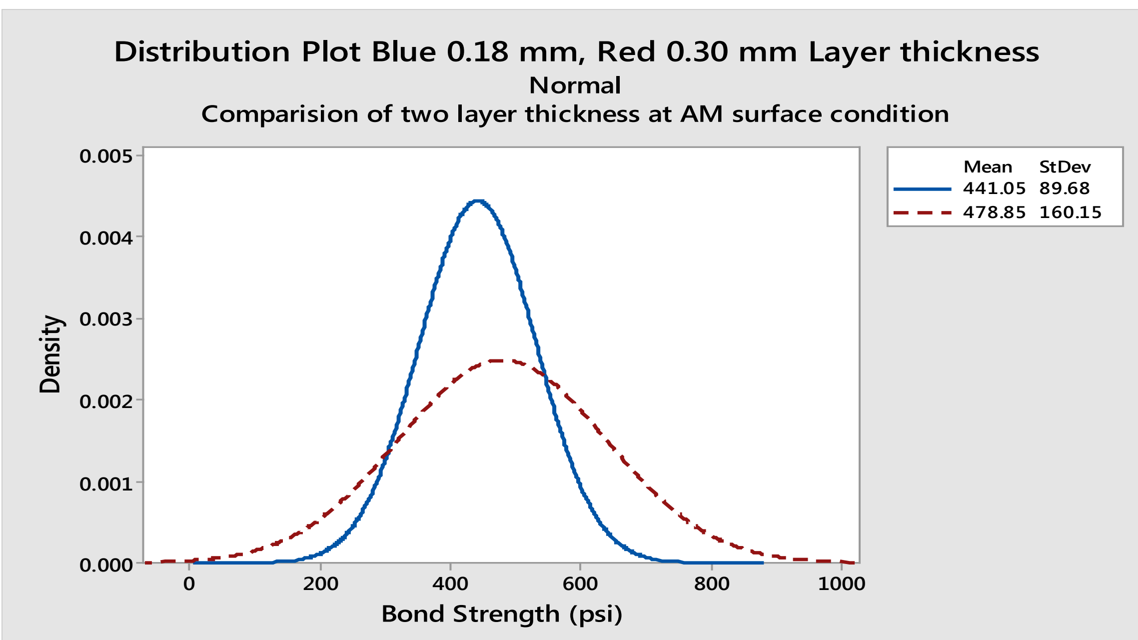

Figure 5.4. Distribution plot for means of 0.18, 0.30 mm layer thickness with AM surface condition

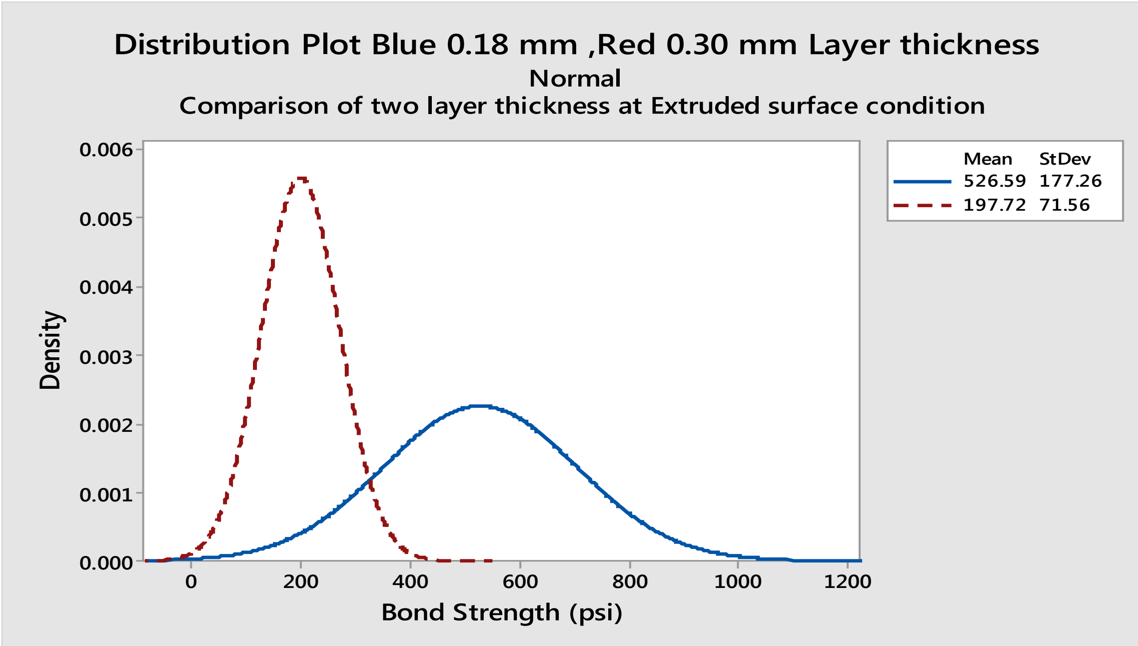

Figure 5.5. Distribution plot for means of 0.18, 0.30 mm layer thickness with extruded surface conditions

The factors which showed significant effect on the bond strength are shown in the normal plot of the standardized effects (Figure 5.6). The interaction between layer thickness and surface roughness had a maximum effect followed by surface roughness and layer thickness.

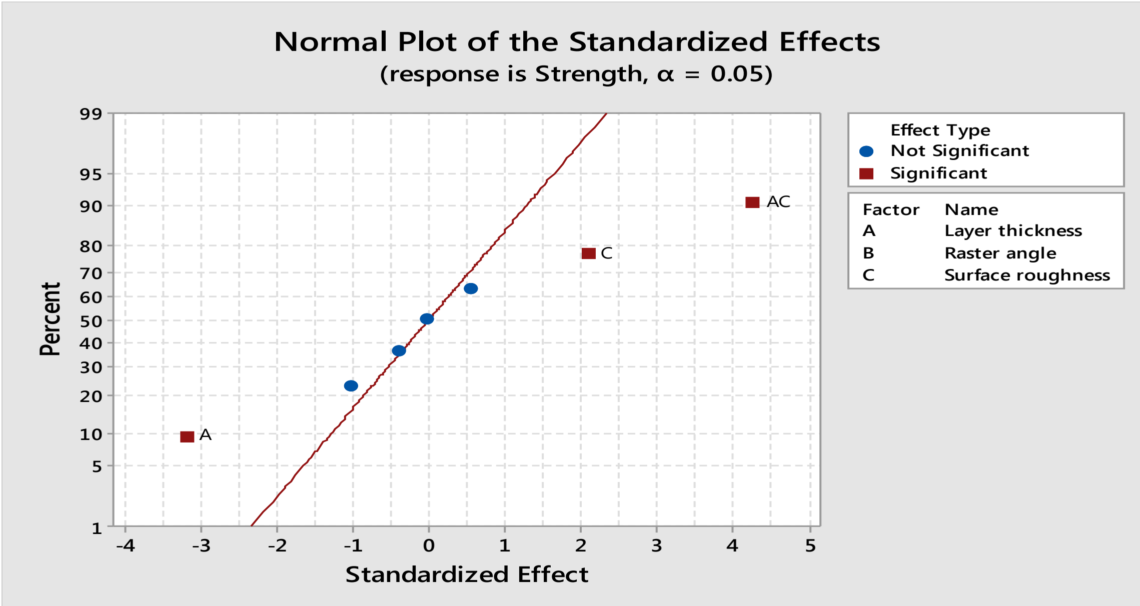

Figure 5.6. Normality plot

From the ANOVA Table 5.2, the effect of factors on the response was confirmed. The main effects of layer thickness and surface condition were highly significant (Table 5.3). Both factors have P-values of 0.003 and 0.043 respectively. At a significance level of 95 %, it can be concluded that these factors have a considerable effect on the strength of the bond formed. From the p-value, it was found that the interaction between layer thickness and surface roughness was highly significant. The residual plots and ANOVA analysis are shown in Appendix G. The percentage of variation in the response was indicated by the R^2 value, which is 51.72% for bond strength.

Table 5.2. Analysis of variance table

Source	**DOF**	**SS**	**Adj MS**	**F**	**p-value**	**Significant**
Layer thickness	1	197509	197509	10.15	0.003	Yes
Raster angle	1	2877	2877	0.15	0.703	No
Surface condition	1	86107	86107	4.42	0.043	Yes
Layer thickness*Raster angle	1	5785	5785	0.30	0.589	No
Raster angle * surface condition	1	20259	20259	1.04	0.315	No
Layer thickness* Surface condition	1	354712	354712	18.22	0.000	Yes
Layer thickness *Raster angle * surface condition*	1	21	21	0.00	0.974	No
Residual Error	32	622932	19467			
Total	39	1290203				

Table 5.3. Main and interactions effects

Process Parameter	Effect	Coefficient	P-value
Layer thickness	-140.5	-70.3	0.003
Raster angle	-17	-8.5	0.703
Surface Roughness	92.8	46.4	0.043
Layer thickness * Raster angle	24.1	12	0.589
Layer thickness * Surface Roughness	188.3	94.2	0.000
Raster angle * Surface Roughness	-45.0	-22.5	0.315

The main effect plots showing the mean strength values were used to study the effect of different layers of thickness, surface roughness, and raster angles, on bond strength of the specimen. The main effects plot in Figure 5.7 shows the difference between two levels of the layer thickness, raster angle, and surface condition factors. It also provides information on the mean of strength based on the aforementioned factors. Analysis of the main effects plot indicates that layer thickness and surface roughness significantly affected the bond strength at a confidence level of 95%.

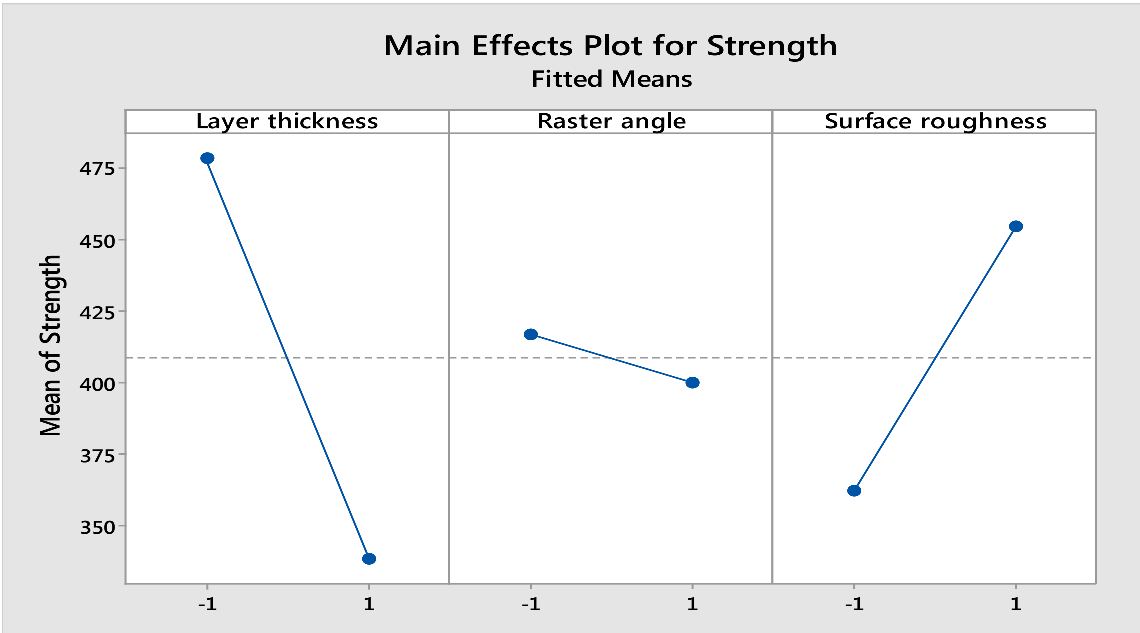

Figure 5.7. Main effects plot for bond strength

For a layer thickness of 0.18 mm, bond strength increases by 141 psi relative to a larger thickness of 0.30 mm, as shown in Figure 5.7. One possible reason for this is that, with smaller layer thickness, the number of beads deposited increases, which concomitantly increases the heat flow between the substrate and the heated extruder. As per literature, the bond formation between layers in AM depends on the temperature. Since the surface of the substrate is not pre-heated, the amount of heat transferred from the extruder to the substrate determines the strength of the bond formed. Therefore, contact time between the extruder and the substrate aids in heating/softening the substrate surface.

A two sample T-test indicated that layer thickness has no effect on bond strength in the case of AM substrates. The reason for discrepancies in bond strength with respect to different layer thicknesses can be attributed to the surface roughness of the substrate. In the case of lower surface roughness, material flow into valleys was limited indicating that heat and contact time of extruder with surface plays a significant role in the bonding process. Conversely, with higher surface roughness, molten material flowed freely into the substrate valleys irrespective of the heat on the substrate indicating that the layer thickness had a negligible effect.

The higher surface roughness of 1034 µin increased the bond strength by 98 psi relative to a lower surface roughness of 10.7 µin. As suggested previously, the surface condition has a definite role to play in the bonding process. A higher surface roughness allowed molten material to flow deep into the valleys thereby implying that the contact area between the substrate surface and molten material increases in turn increasing the magnitude of the load to break the sample. On the contrary, for a lower surface roughness the contact angle of the molten material with the solid substrate was low. Figure 5.8 shows that the contact area between the molten material and a smooth surface is low when compared the same with a rough surface.

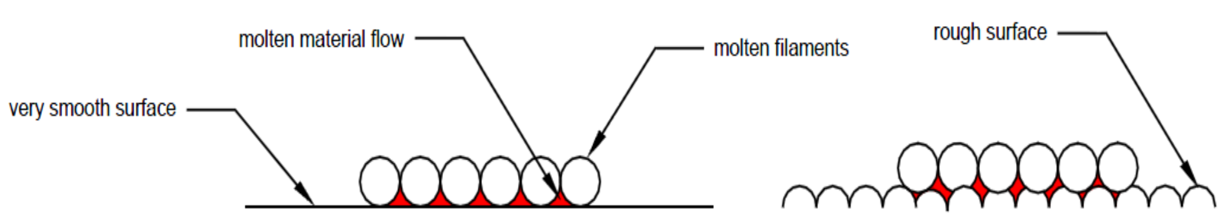

Figure 5.8. Molten material flow into different surface conditions

The effect of raster angle on bond strength is negligible. The directions in which beads are deposited have no significant effect on strength of the bond formed because of the flow of material into the voids. Therefore the effect of direction of deposition was comparatively lower than the other factors considered in this research.

Interaction and effects plots are inserted in the factorial plots. From the interactions plots in Figure 5.9 it was found that the raster angle had almost no interaction with surface condition or layer thickness. However, there was strong interaction between layer thickness and surface roughness.

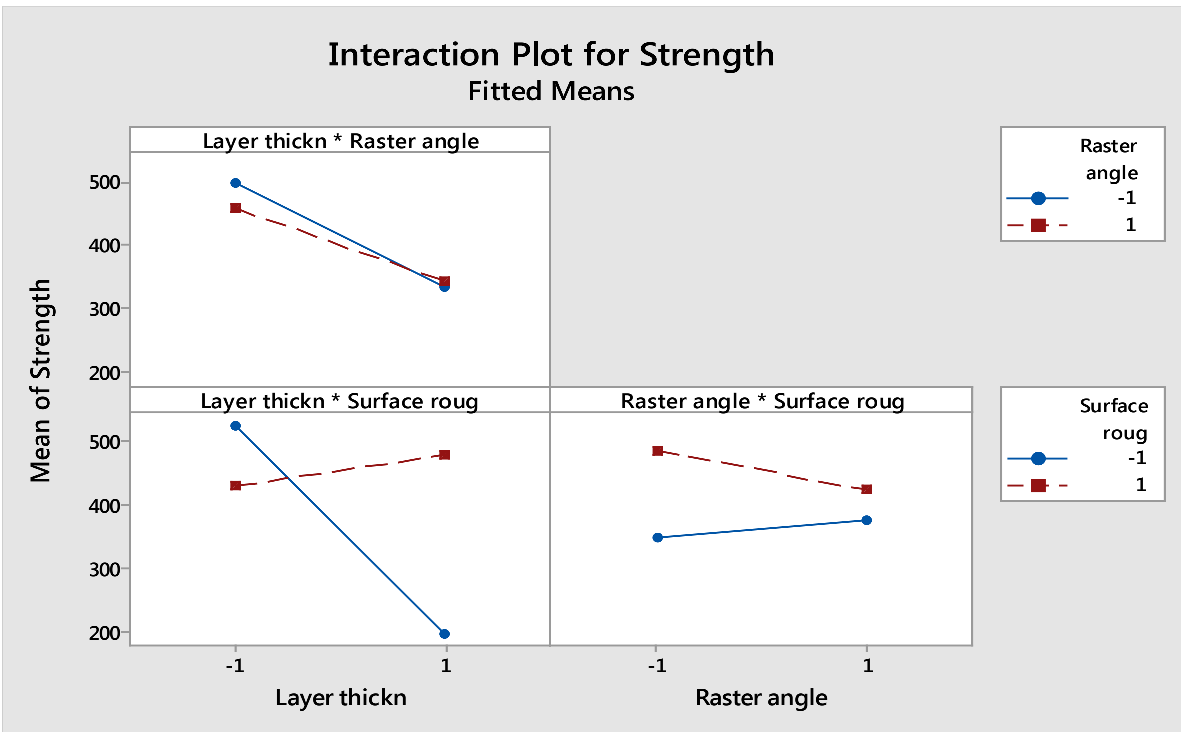

Figure 5.9. Interaction plot for bond strength

A linear regression model was developed to predict the bond strength as a function of layer thickness, surface roughness and the interaction between layer thickness and surface roughness:

$$\boldsymbol{\sigma} = \mathbf{46.4}\,\boldsymbol{z} - \mathbf{70.3}\,\boldsymbol{x} + \mathbf{94.2}\,\boldsymbol{x} * \boldsymbol{z} + \mathbf{408.6}$$

where σ is the bond strength, x is the layer thickness, and z is the surface roughness. Since raster angle had no effect on the bond strength this factor was dropped from the prediction model. Minitab 17 was used to perform these calculations, and from the effects model it was found that the layer thickness had a negative effect. This means that having a greater surface roughness and lower thickness helps in achieving a better bond strength.

5.3 Regression analysis

Additional full factorial experiments were conducted after adding an extra level to the layer thickness and surface roughness. Each condition was replicated five times. Regression analysis was used to develop a model with main effects and second-order quadratic terms. It was found from the analysis that the quadratic term of layer thickness has a very large P-value and hence had no significant effect on bond strength. A model was fit after dropping the quadratic layer thickness term. Residual plots and Minitab 17 output are shown in Appendix H. Table 5.4 shows all significant terms after performing regression analysis.

Table 5.4. Analysis of variance table after dropping the insignificant squared term

Source	**DOF**	**SS**	**Adj MS**	**F**	**p-value**	**Significant**
Layer thickness	1	432541	432541	20.20	0.000	Yes
Surface roughness	1	81009	81009	3.78	0.059	Yes
Surface Roughness * Surface Roughness	1	379090	379090	17.70	0.000	Yes
Layer thickness* Surface Roughness	1	89323	89323	4.17	0.048	Yes
Error	40	856527	21413			
Lack-of-Fit	38	854783	22494	25.79	0.038	
Pure Error	2	1744	872			
Total	44	24859545				

5.4 Prediction model

ANOVA Table 5.4 summarizes the main effects, in terms of the square of the surface roughness and interaction for response analysis via regression. A regression model was developed as a function of bond strength, layer thickness, surface roughness, quadratic term of surface roughness, and the interaction between layer thickness and surface roughness:

$$\boldsymbol{\sigma = 0.647\, z - 3437\, x - 0.000850\, z^2 + 0.208\, x * z + 1087}$$

The percentage of variation in the response was indicated by the R^2 value, which is 65.55% for bond strength. The contour plot shown in Figure 5.10 indicates that the direction of improvement is towards the lower bound of layer thickness. Also, the optimum value for surface roughness lies between 300 to 900 µin. Practically, it is not possible to use less than a 0.1 mm layer thickness considering the fabrication time for a part. Hence, a constraint was put in place to ensure that the thickness exceeds this level, which thereby improved the bond strength considerably. Solver in Microsoft excel was used to optimize the regression equation. It was found that the bond strength value of 958psi was obtained at an optimized surface roughness value of 503µin and layer thickness of 0.1 mm.

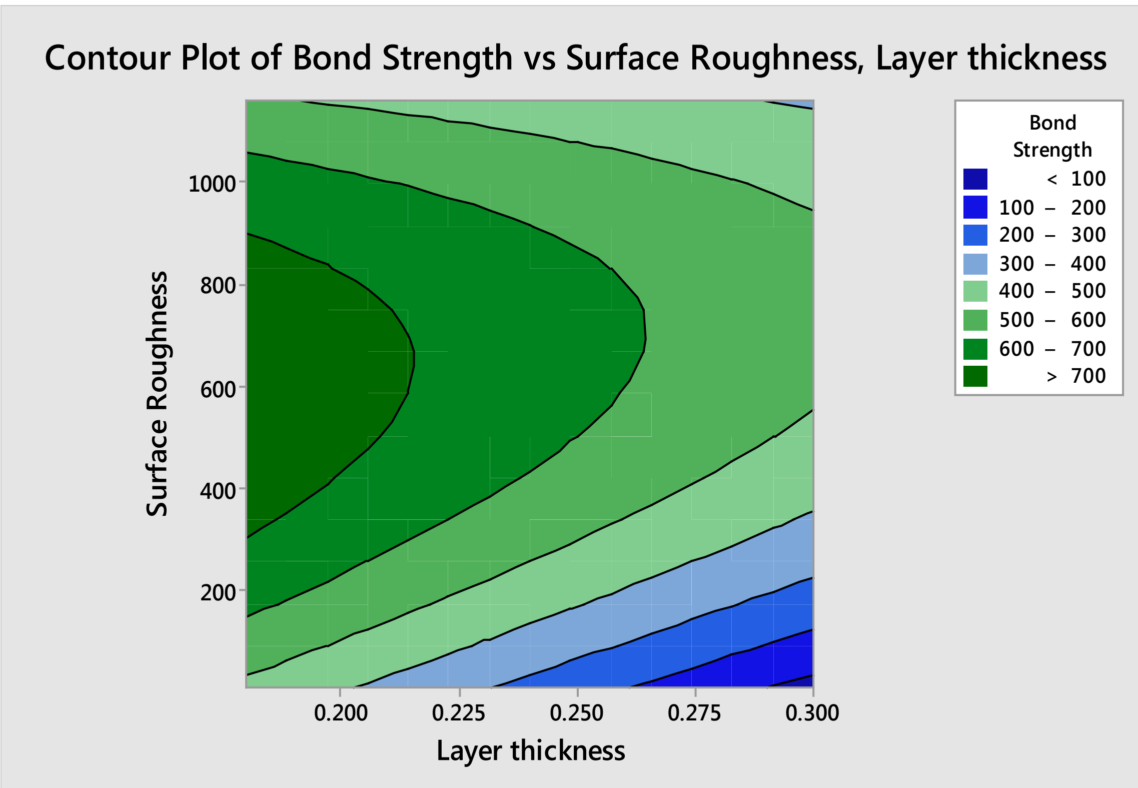

Figure 5.10. Contour plot illustrating the direction of improvement

Experimental data can be represented by a response surface plot, as shown in Figure 5.11. The surface plot shows that bond strength increased between surface roughness ranges of 400-800 µin and decreased as the layer thickness values increased.

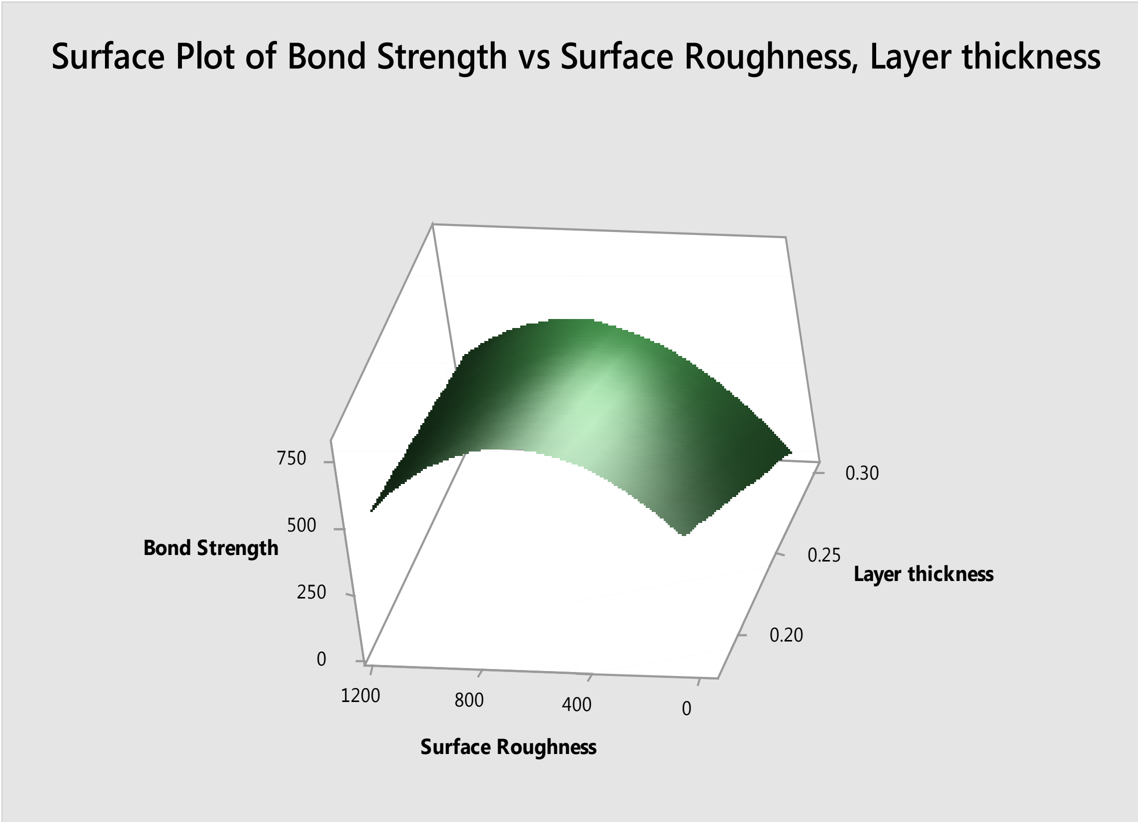

Figure 5.11. Surface plot for bond strength Vs Layer thickness, Surface roughness

5.5 Discussion

The objective of this thesis was to analyze the effect of surface roughness and AM process parameters on adhesion between the substrate and the first layer of the auxiliary part. It has been shown by adhesion theory that surface roughness influences bond strength for adhesives. However, this theory has not been verified in the case of AM while joining two surfaces. Real-time analysis of bond strength while printing on an existing substrate has not been evaluated in the AM literature. This research proves our hypothesis that surface roughness of the substrate and the layer thickness selected for printing the auxiliary part both play a significant role in improving the bond strength.

Using full factorial screening experiments it was found that layer thickness and surface roughness have significant effect on bond strength. A p-value of 0.043 for surface roughness and 0.003 for layer thickness at 95% confidence interval indicates that both factors affect bond strength. From the distribution plots it is found that substrates with a higher surface roughness demonstrated higher bond strength. The results of regression analysis after adding additional levels indicate the possibility for molten material to flow into the valleys on the surface. An optimum R_a was found to be 503µin obtained by optimizing the regression equation. Also, as the layer thickness decreases, bond strength increases. One possible reason for the difference in strength arising from layer thickness values can be attributed to the heat flow from the extruder onto substrate surface; however there may be some other reasons which are to be examined in detail with further analysis.

The optimized process parameters that were obtained from the results of additional full factorial experiments can be used to improve the mechanical strength of parts embedded with circuits that are printed using 5/6 axis printers. This research also provides a greater insight into the significant AM process parameters and their values that can be used directly in the case of re-printing and patching processes. Furthermore, this study helps manufacturers to definitively decide on the need for post-processing operations on existing parts before patching them with a complex design, thereby reducing the cost and time to fabricate customized components.

6. Conclusions

From the full factorial experimental study, we can summarize that the factors that have a significant effect on bond strength in the case of re-manufacturing/patching process have been identified. A regression model has been developed based on the experiments that were conducted with additional levels of layer thickness and surface roughness. Contour and surface plots were generated from the data that was collected. Microsoft Excel solver was used to optimize the regression model to find the layer thickness and surface roughness values that yield maximum bond strength.

6.1 Summary

Surface roughness and layer thickness are found to have a significant effect on strength. It was found that that the bond formed on substrates with a surface roughness of 503 µin and 0.1 mm layer thickness yields optimized bond strength of 958 psi. The contour plot indicates that the region of improvement is between 300 to 900 µin for surface roughness and 0.22 to 0.1 mm for layer thickness. Based on the analysis we can conclude that interaction between surface roughness and layer thickness has considerably stronger influence on bond strength than the independent factors. On the other hand, bond strength is not affected by the angle at which rasters are deposited on the top of substrates.

6.2 Contributions of the work

This work finds application in the area of patching/re-manufacturing where parts are joined together using AM process. This research represents a first step towards understanding bond strength in such circumstances, allowing manufacturers to intelligently select process parameters for the production of both the substrate and the added geometry. The major limitation in AM, stair stepping can be reduced to some extent by using the procedure used for this research i.e. by halting the printing process and changing the build orientation of the print. Bond strength of the final part can be predicted using the regression model before printing the component. Process parameters can be selected based on the type of application being manufactured.

6.3 Recommendations

In this research, an attempt was made to examine the bond strength of a part which was patched/re-manufactured using AM process. Constrained by the availability of resources and time, only a few factors were considered for the screening and follow up experiments. This research can be extended further by considering additional process parameters like infill percentage, printing speed, and substrate temperature prior to patching. Investigating these factors would help in determining techniques that improve bond strength and reduce the fabrication time. This further helps in building a robust model where more variables can be taken into consideration, which in turn would help improve the process.

There is very little literature available on evaluation of bond strength in patching/re-manufacturing using AM and this research is, to the best of the author's knowledge, the first to address this problem. Due to the lack of an estimate for variance from previous experiments it was difficult to decide on the number of replications for each experimental condition. Increasing the number of replications and testing will help in providing additional evidence to validate and further improve the results.

It was found that first layer height plays a crucial role in bond formation process. However, the underlying phenomenon behind it is still unexplored. Depositing a single layer on top of a substrate and microscopic investigation of that bond can help gain better insight into the physics of bond formation in the negative 1st layer deposition method.

APPENDIX A

3-view drawings for specimens

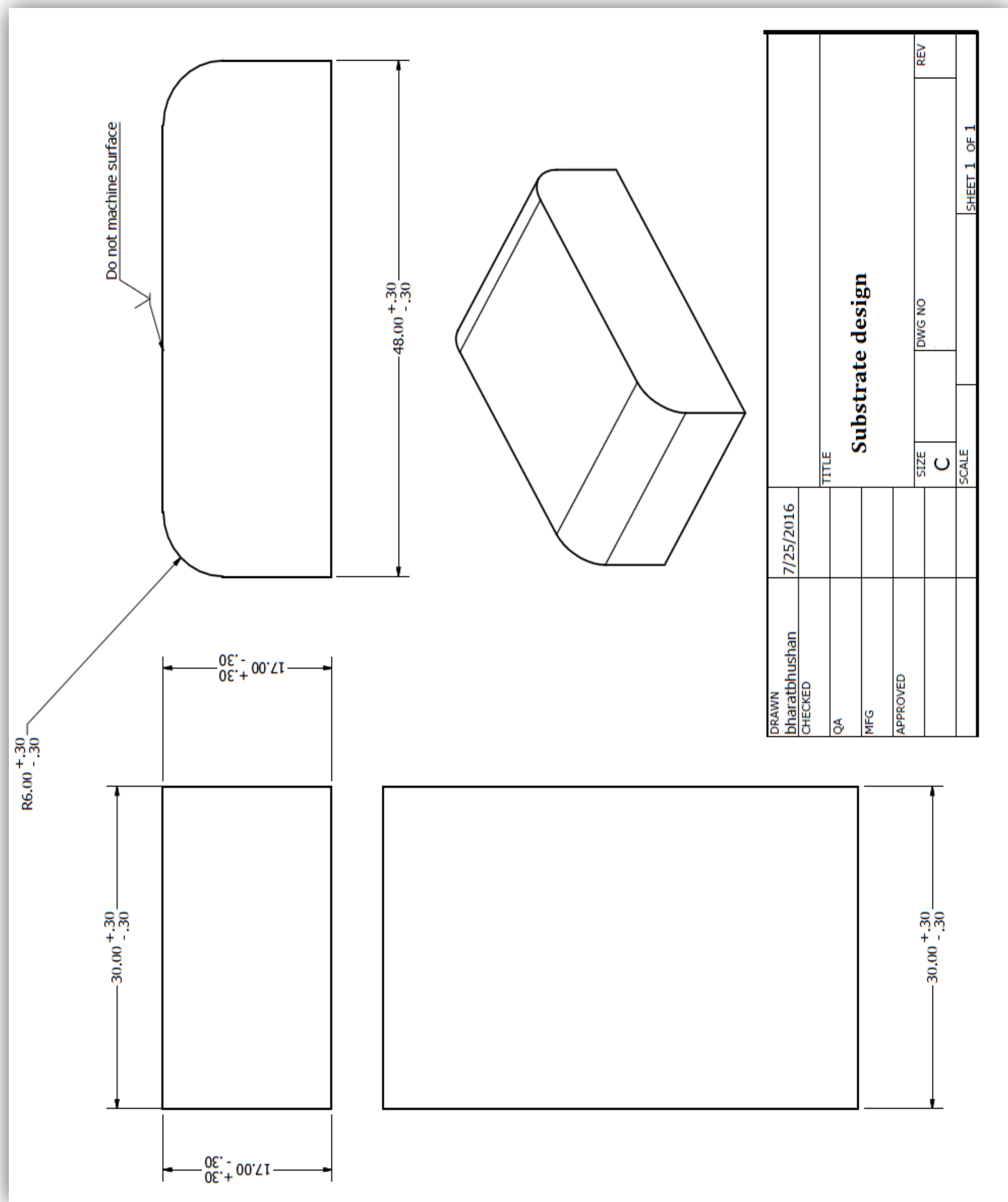

Do not machine surface
48.00 +.30 -.30
R6.00 +.30 -.30
17.00 +.30 -.30
30.00 +.30 -.30
17.00 +.30 -.30
30.00 +.30 -.30
DRAWN
bharatbhushan
7/25/2016
CHECKED
QA
MFG
APPROVED
TITLE
Substrate design
SIZE
C
DWG NO
REV
SCALE
SHEET 1 OF 1

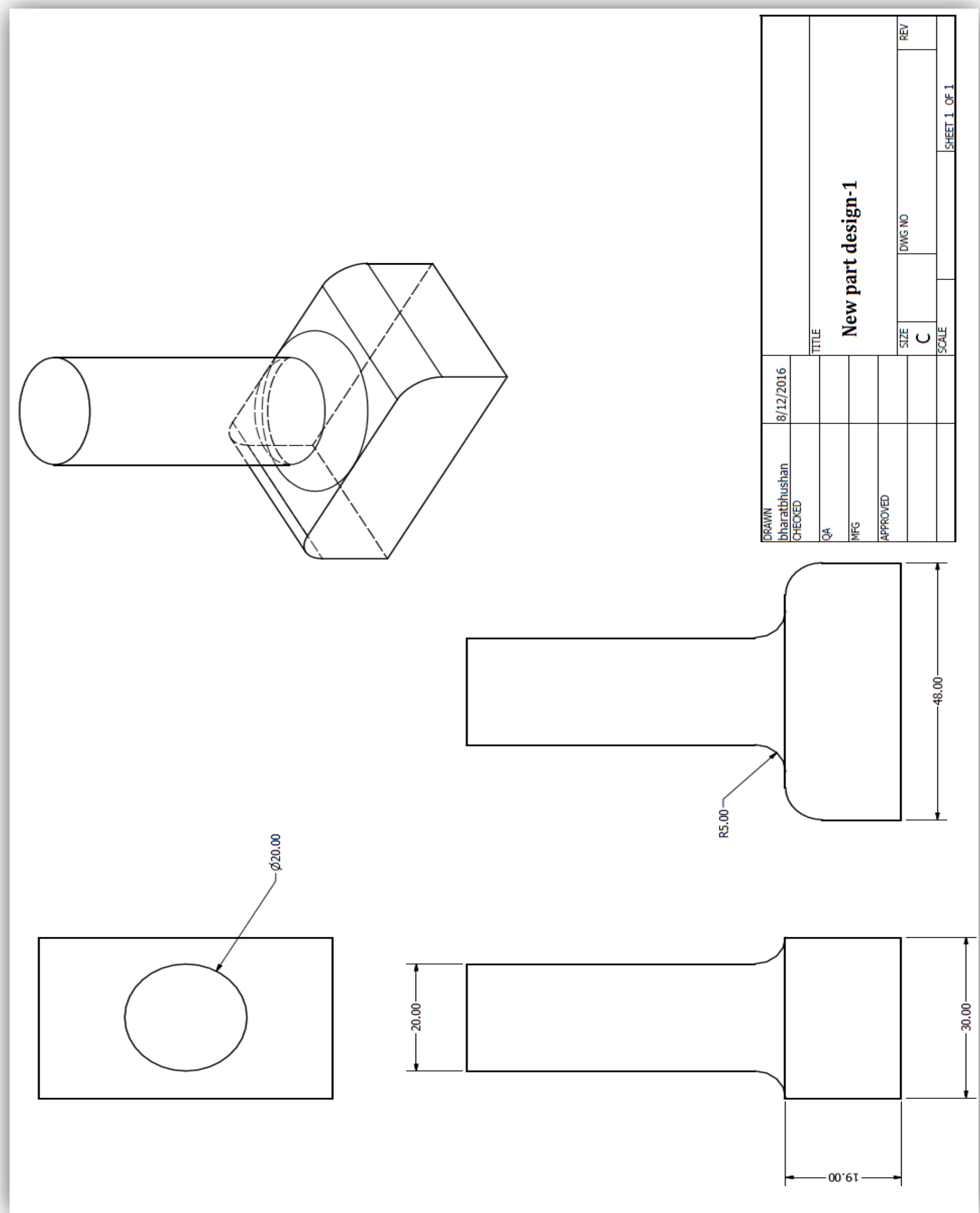
DRAWN
bharatbhushan
8/12/2016
CHECKED
QA
MFG
APPROVED
TITLE
New part design-1
SIZE
C
DWG NO
REV
SCALE
SHEET 1 OF 1
48.00
R5.00
Ø20.00
20.00
30.00
19.00

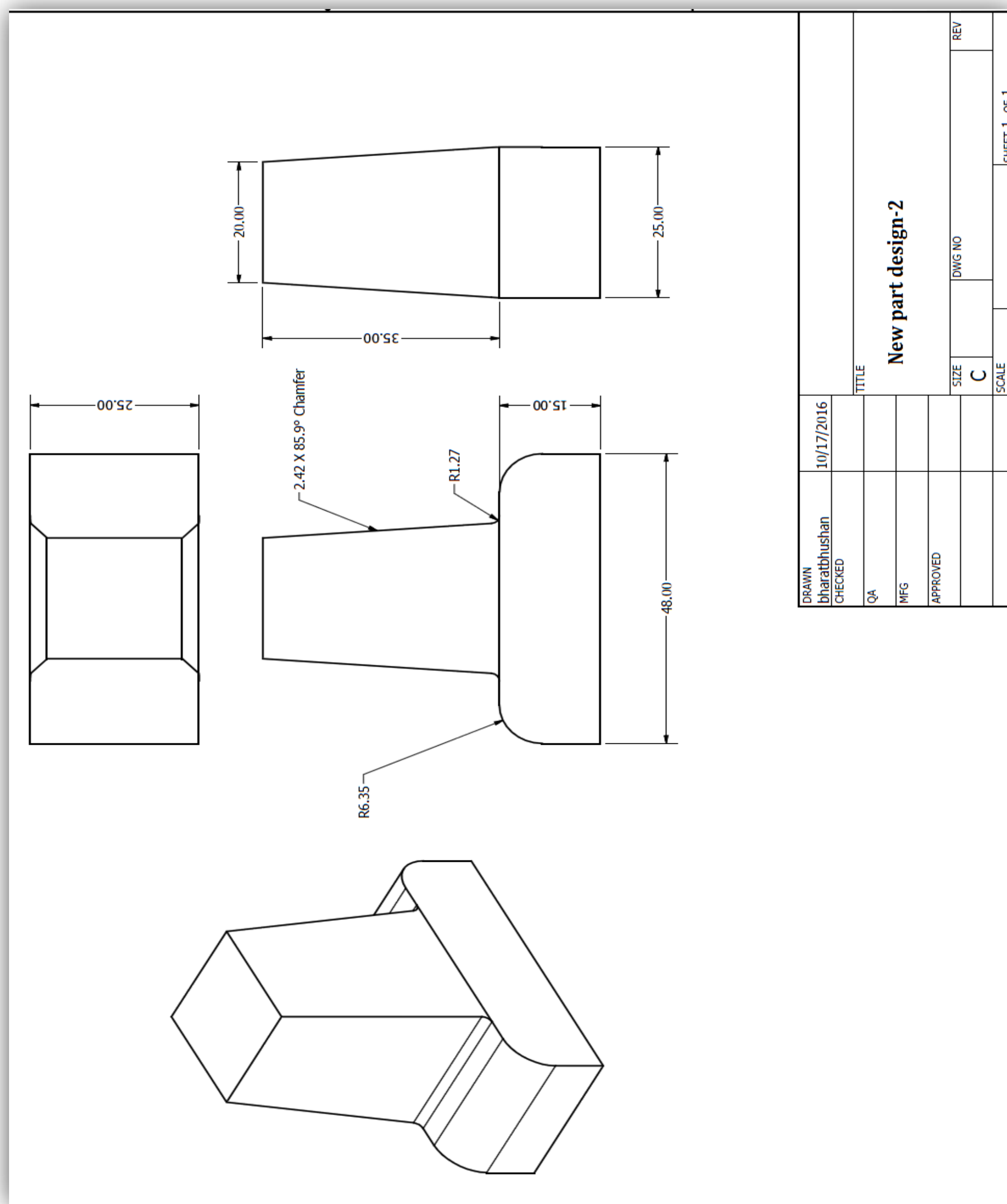
20.00
25.00
35.00
25.00
15.00
48.00
2.42 X 85.9° Chamfer
R1.27
R6.35
DRAWN
bharatbhushan
10/17/2016
CHECKED
QA
MFG
APPROVED
TITLE
New part design-2
SIZE
C
DWG NO
REV
SCALE
SHEET 1 OF 1

APPENDIX B

Surface roughness values of substrates

Substrate for full factorial exp.	**Surface condition**	**Average Surface Roughness value (Ra) µin**
82	45 stair step	1041.5
53	45 stair step	1024.3
71	45 stair step	1010.6
49	45 stair step	1003.2
72	45 stair step	1033.4
48	45 stair step	1009.3
74	45 stair step	1058.8
52	45 stair step	1018.4
50	45 stair step	1011.3
47	45 stair step	1025.8
69	45 stair step	1015.1
68	45 stair step	1012.8
57	45 stair step	958.93
75	45 stair step	1113.3
81	45 stair step	1137.7
54	45 stair step	1026.8
55	45 stair step	1013.1
56	45 stair step	1017.9
51	45 stair step	1009.1
70	45 stair step	1141.6
61	Machined	10.3
60	Machined	10.61
76	Machined	10.22
77	Machined	12.31
64	Machined	9.01
80	Machined	11.62
59	Machined	11.06
36	Machined	9.41
40	Machined	9.81
45	Machined	10.95
78	Machined	11.48
63	Machined	12.25
66	Machined	10.81
39	Machined	12.51
42	Machined	10.54
62	Machined	9.3
67	Machined	9.42
43	Machined	11.91
83	Machined	10.67

34	Machined	9.93

Substrate for RSM exp.	**Surface condition**	**Average Surface Roughness value (Ra) µin**
13	Z direction built	777.673
14	Z direction built	720.08
15	Machined	12.47
16	Machined	11.48
17	Machined	11.51
18	Machined	11.93
19	Machined	11.38
20	Z direction built	814.443
21	Z direction built	786.46
22	Z direction built	799.64
23	Z direction built	794.483
24	Z direction built	797.147
25	Z direction built	798.137
26	Z direction built	798.457
27	Z direction built	776.847
28	Z direction built	793.283
30	Z direction built	812.16
31	Z direction built	805.87
32	Z direction built	795.39
33	45 stair step	1116.43
34	45 stair step	1151.23
35	45 stair step	1121.93
36	45 stair step	1125.57
37	45 stair step	1159.27
38	Z direction built	795.63
39	Z direction built	772.02

APPENDIX C

Mechanical drawings of grips for tensile testing

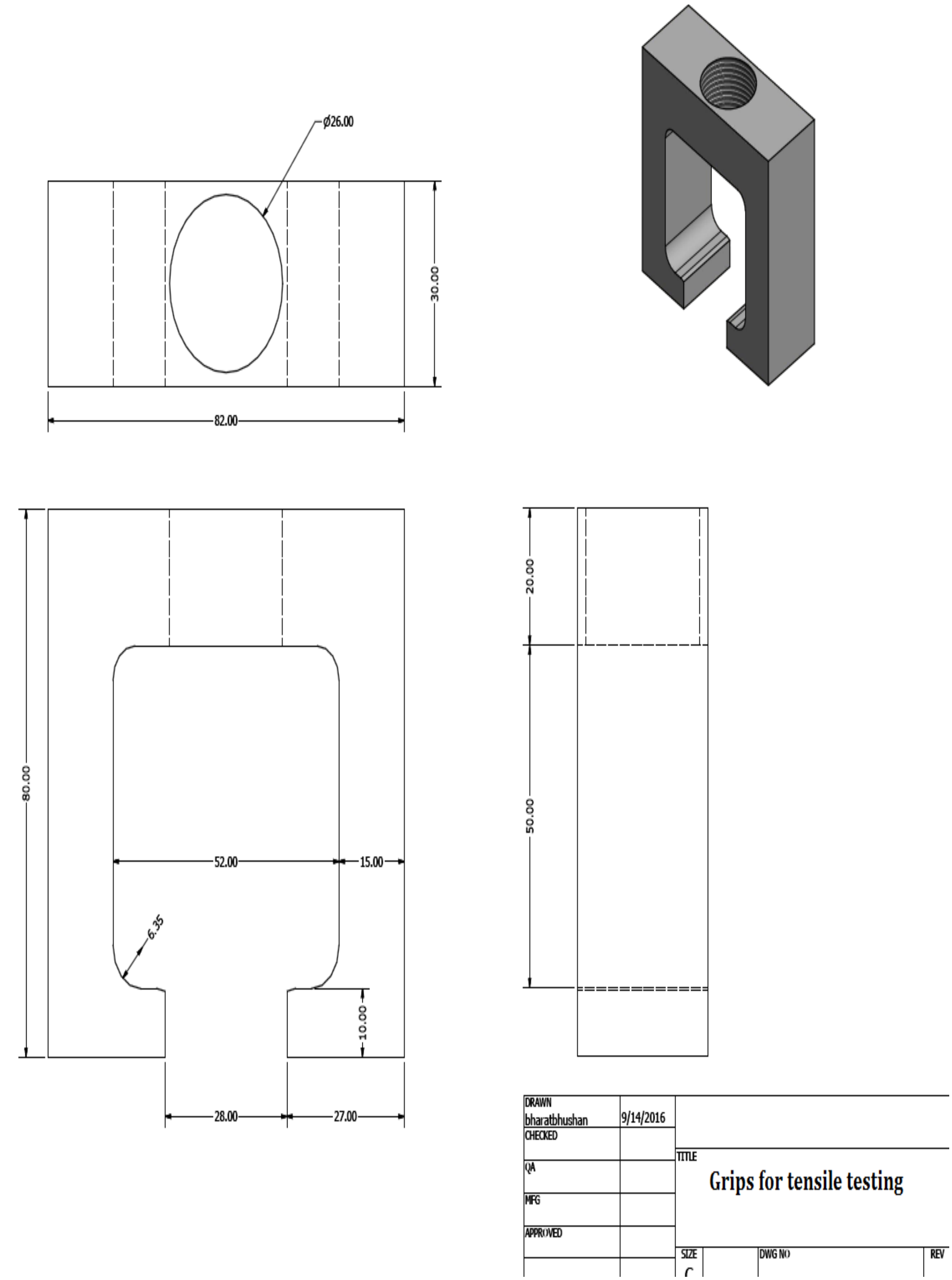

ϕ26.00
30.00
82.00
80.00
52.00
15.00
6.35
10.00
28.00
27.00
20.00
50.00
DRAWN
bharatbhushan
9/14/2016
CHECKED
QA
MFG
APPROVED
TITLE
Grips for tensile testing
SIZE
C
DWG NO
REV

APPENDIX D

Data for one replication of 1^{st} layer height experiments

Positive 1st layer height				
Condition	**Raster angle**	**Layer thickness**	**Surface Roughness**	**Strength**
1	0	0.3	1034.14	68.54
2	90	0.3	1034.14	40.98
3	0	0.3	10.7	17.1
4	90	0.3	10.7	0
5	0	0.18	1034.14	0
6	90	0.18	1034.14	64.61
7	0	0.18	10.7	0
8	90	0.18	10.7	80.92

Negative 1st layer height				
Condition	**Raster angle**	**Layer thickness**	**Surface Roughness**	**Strength**
1	0	0.3	1034.14	663.14
2	90	0.3	1034.14	639.51
3	0	0.3	10.7	237.96
4	90	0.3	10.7	336.3
5	0	0.18	1034.14	588.32
6	90	0.18	1034.14	509.58
7	0	0.18	10.7	635.58
8	90	0.18	10.7	643.45

APPENDIX E

Design matrix for experimental runs generated from Minitab-17

StdOrder	RunOrder	CenterPt	Blocks	layer thickness	raster angle	surface cond.	strength
10	1	1	1	1	-1	-1	
14	2	1	1	1	-1	1	
2	3	1	1	1	-1	-1	
28	4	1	1	1	1	-1	
3	5	1	1	-1	1	-1	
9	6	1	1	-1	-1	-1	
32	7	1	1	1	1	1	
16	8	1	1	1	1	1	
40	9	1	1	1	1	1	
35	10	1	1	-1	1	-1	
1	11	1	1	-1	-1	-1	
36	12	1	1	1	1	-1	
20	13	1	1	1	1	-1	
30	14	1	1	1	-1	1	
18	15	1	1	1	-1	-1	
22	16	1	1	1	-1	1	
11	17	1	1	-1	1	-1	
26	18	1	1	1	-1	-1	
7	19	1	1	-1	1	1	
27	20	1	1	-1	1	-1	
13	21	1	1	-1	-1	1	
12	22	1	1	1	1	-1	
25	23	1	1	-1	-1	-1	
15	24	1	1	-1	1	1	
39	25	1	1	-1	1	1	
19	26	1	1	-1	1	-1	
38	27	1	1	1	-1	1	
17	28	1	1	-1	-1	-1	
29	29	1	1	-1	-1	1	
6	30	1	1	1	-1	1	
4	31	1	1	1	1	-1	
31	32	1	1	-1	1	1	
33	33	1	1	-1	-1	-1	
37	34	1	1	-1	-1	1	
21	35	1	1	-1	-1	1	
8	36	1	1	1	1	1	
23	37	1	1	-1	1	1	
24	38	1	1	1	1	1	
34	39	1	1	1	-1	-1	
5	40	1	1	-1	-1	1	

APPENDIX F

Graphical Summary & normality test

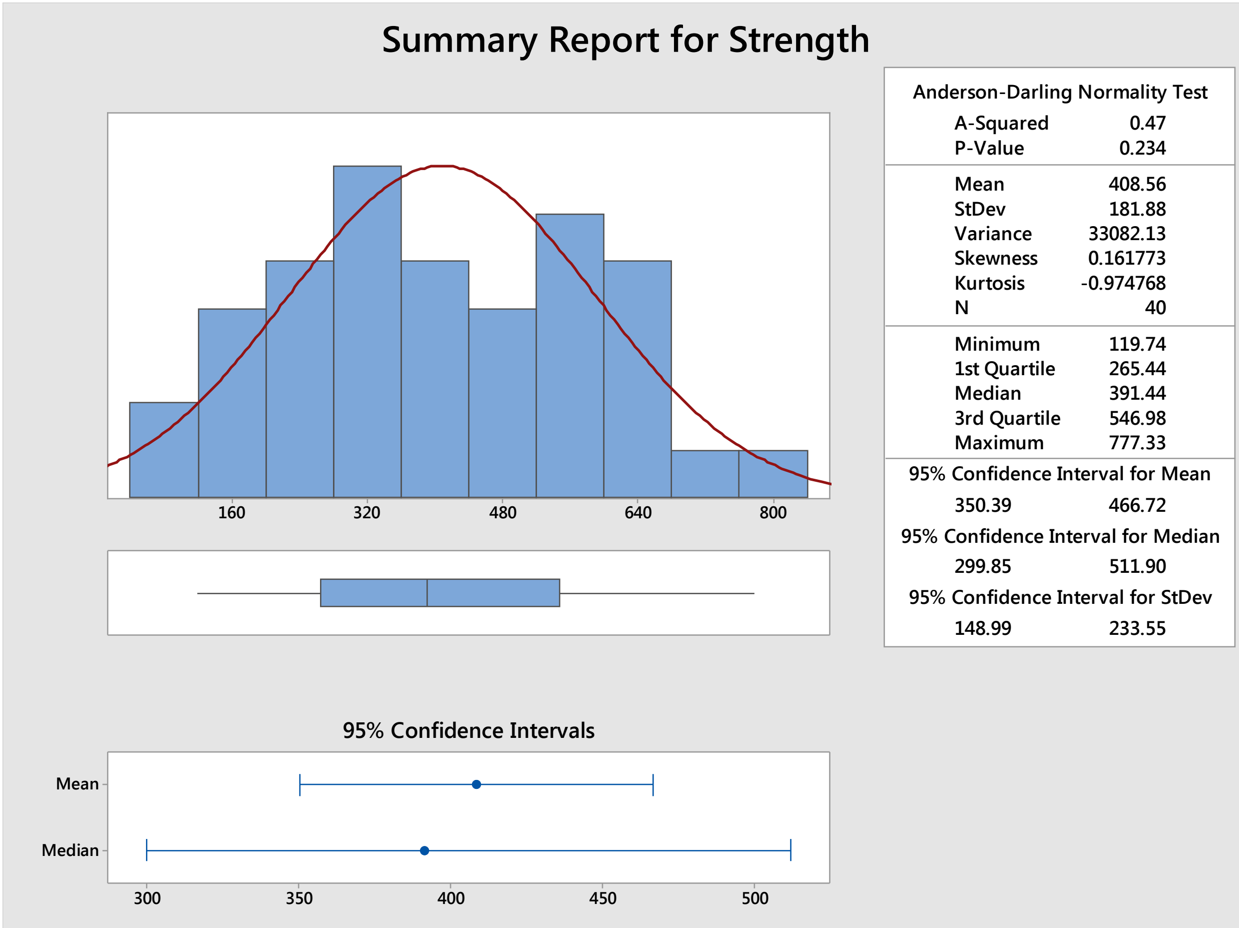
Summary Report for Strength
Anderson-Darling Normality Test
A-Squared 0.47
P-Value 0.234
Mean 408.56
StDev 181.88
Variance 33082.13
Skewness 0.161773
Kurtosis -0.974768
N 40
Minimum 119.74
1st Quartile 265.44
Median 391.44
3rd Quartile 546.98
Maximum 777.33
95% Confidence Interval for Mean
350.39 466.72
95% Confidence Interval for Median
299.85 511.90
95% Confidence Interval for StDev
148.99 233.55
160
320
480
640
800
95% Confidence Intervals
Mean
Median
300
350
400
450
500

APPENDIX G

Minitab-17 results for full factorial statistical analysis

Anova results, coefficients, and residual plots

Analysis of Variance

Source	DF	Adj SS	Adj MS	F-Value	P-Value
Model	7	667271	95324	4.90	0.001
Linear	3	286494	95498	4.91	0.006
Layer thickness	1	197509	197509	10.15	0.003
Raster angle	1	2877	2877	0.15	0.703
Surface roughness	1	86107	86107	4.42	0.043
2-Way Interactions	3	380756	126919	6.52	0.001
Layer thickness*Raster angle	1	5785	5785	0.30	0.589
Layer thickness*Surface roughness	1	354712	354712	18.22	0.000
Raster angle*Surface roughness	1	20259	20259	1.04	0.315
3-Way Interactions	1	21	21	0.00	0.974
Layer thickness*Raster angle*Surface roughness	1	21	21	0.00	0.974
Error	32	622932	19467		
Total	39	1290203			

Model Summary

S	R-sq	R-sq(adj)	R-sq(pred)
139.523	51.72%	41.16%	24.56%

Coded Coefficients

Term	Effect	Coef	SE Coef	T-Value	P-Value
Constant		408.6	22.1	18.52	0.000
Layer thickness	-140.5	-70.3	22.1	-3.19	0.003
Raster angle	-17.0	-8.5	22.1	-0.38	0.703
Surface roughness	92.8	46.4	22.1	2.10	0.043
Layer thickness*Raster angle	24.1	12.0	22.1	0.55	0.589
Layer thickness*Surface roughness	188.3	94.2	22.1	4.27	0.000
Raster angle*Surface roughness	-45.0	-22.5	22.1	-1.02	0.315
Layer thickness*Raster angle*Surface roughness	-1.4	-0.7	22.1	-0.03	0.974

Regression Equation in Uncoded Units

Strength = 408.6 - 70.3 Layer thickness - 8.5 Raster angle + 46.4 Surface roughness
+ 12.0 Layer thickness*Raster angle+ 94.2 Layer thickness*Surface roughness
- 22.5 Raster angle*Surface roughness -
0.7 Layer thickness*Raster angle*Surface roughness

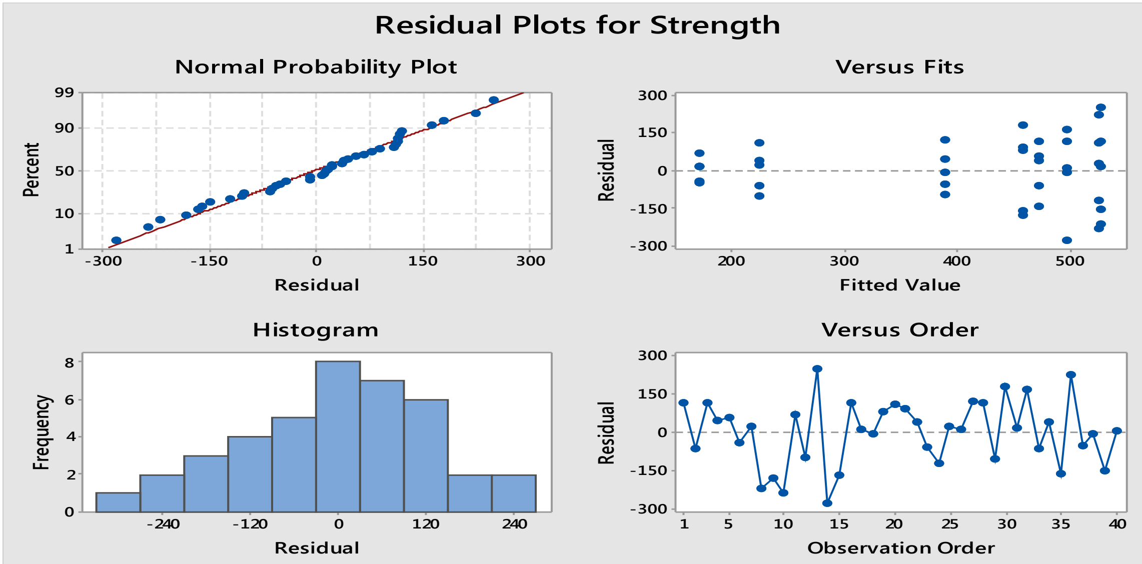

Model fitting with significant terms

Analysis of Variance

Source	DF	Adj SS	Adj MS	F-Value	P-Value
Model	3	638329	212776	11.75	0.000
Linear	2	283617	141808	7.83	0.002
Layer thickness	1	197509	197509	10.91	0.002
Surface roughness	1	86107	86107	4.76	0.036
2-Way Interactions	1	354712	354712	19.59	0.000
Layer thickness*Surface roughness	1	354712	354712	19.59	0.000
Error	36	651875	18108		
Lack-of-Fit	4	28942	7236	0.37	0.827
Pure Error	32	622932	19467		
Total	39	1290203			

Model Summary

S	R-sq	R-sq(adj)	R-sq(pred)
134.565	49.48%	45.26%	37.62%

Coded Coefficients

Term	Effect	Coef	SE Coef	T-Value	P-Value	VIF
Constant		408.6	21.3	19.20	0.000	
Layer thickness	-140.5	-70.3	21.3	-3.30	0.002	1.00
Surface roughness	92.8	46.4	21.3	2.18	0.036	1.00
Layer thickness*Surface roughness	188.3	94.2	21.3	4.43	0.000	1.00

Regression Equation in Uncoded Units

Strength = 408.6 - 70.3 Layer thickness + 46.4 Surface roughness
+ 94.2 Layer thickness*Surface roughness

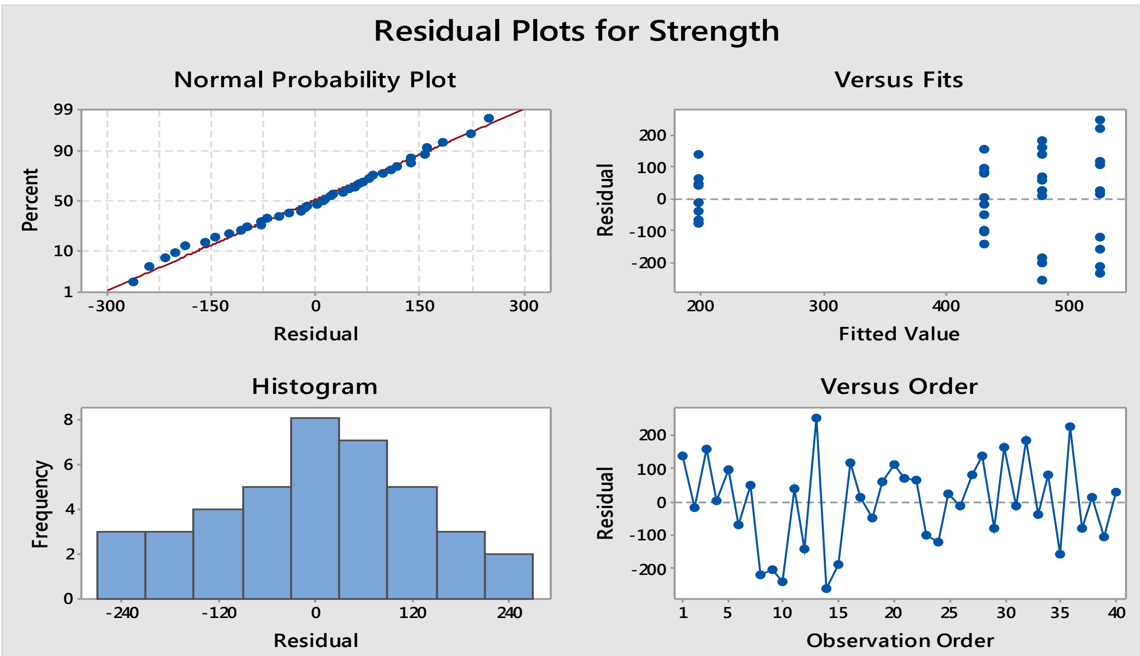

APPENDIX H

Minitab-17 results for regression analysis

Anova results, coefficients, and residual plots

Regression Analysis: Bond Strength versus Layer thickness, Surface Roughness

Analysis of Variance

Source	DF	Adj SS	Adj MS	F-Value	P-Value
Regression	5	1630054	326011	14.86	0.000
Layer thickness	1	2974	2974	0.14	0.715
Surface Roughness	1	81579	81579	3.72	0.061
Layer thickness*Layer thickness	1	636	636	0.03	0.866
Surface Roughness*Surface Roughness	1	373248	373248	17.01	0.000
Layer thickness*Surface Roughness	1	88992	88992	4.06	0.051
Error	39	855892	21946		
Lack-of-Fit	37	854147	23085	26.47	0.037
Pure Error	2	1744	872		
Total	44	2485945			

Model Summary

S	R-sq	R-sq(adj)	R-sq(pred)
148.142	65.57%	61.16%	53.64%

Coefficients

Term	Coef	SE Coef	T-Value	P-Value	VIF
Constant	963	757	1.27	0.211	
Layer thickness	-2356	6400	-0.37	0.715	201.59
Surface Roughness	0.653	0.339	1.93	0.061	47.44
Layer thickness*Layer thickness	-2250	13219	-0.17	0.866	199.15
Surface Roughness*Surface Roughness	-0.000856	0.000207	-4.12	0.000	19.91
Layer thickness*Surface Roughness	2.08	1.03	2.01	0.051	27.99

Regression Equation

Bond Strength = 963 - 2356 Layer thickness + 0.653 Surface Roughness
- 2250 Layer thickness*Layer thickness
- 0.000856 Surface Roughness*Surface Roughness
+ 2.08 Layer thickness*Surface Roughness

Fits and Diagnostics for Unusual Observations

Obs	Bond Strength	Fit	Std Resid	Resid

45	749.8	476.4	273.4	2.03	R

R Large residual

Residual Plots for Bond Strength

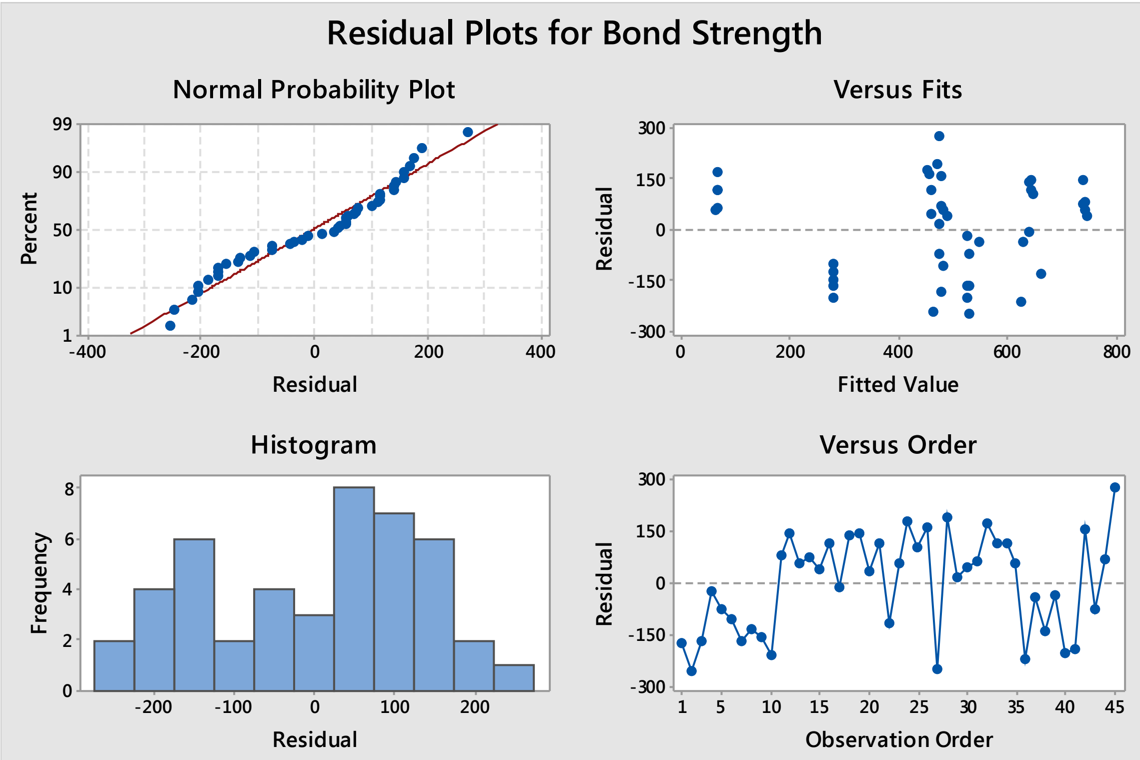

Regression Analysis: Bond Strength versus Layer thickness, Surface Roughness

Analysis of Variance

Source	DF	Adj SS	Adj MS	F-Value	P-Value
Regression	4	1629418	407355	19.02	0.000
Layer thickness	1	432541	432541	20.20	0.000
Surface Roughness	1	81009	81009	3.78	0.059
Surface Roughness*Surface Roughness	1	379090	379090	17.70	0.000
Layer thickness*Surface Roughness	1	89323	89323	4.17	0.048
Error	40	856527	21413		
Lack-of-Fit	38	854783	22494	25.79	0.038
Pure Error	2	1744	872		
Total	44	2485945			

Model Summary

S	R-sq	R-sq(adj)	R-sq(pred)
146.332	65.55%	62.10%	55.76%

Coefficients

Term	Coef	SE Coef	T-Value	P-Value	VIF
Constant	1087	188	5.79	0.000	
Layer thickness	-3437	765	-4.49	0.000	2.95
Surface Roughness	0.647	0.333	1.95	0.059	46.79
Surface Roughness*Surface Roughness	-0.000850	0.000202	-4.21	0.000	19.33
Layer thickness*Surface Roughness	2.08	1.02	2.04	0.048	27.97

Regression Equation

Bond Strength = 1087 - 3437 Layer thickness + 0.647 Surface Roughness
- 0.000850 Surface Roughness*Surface Roughness
+ 2.08 Layer thickness*Surface Roughness

Fits and Diagnostics for Unusual Observations

Obs	Bond Strength	Fit	Resid	Std Resid	
45	749.8	479.2	270.5	2.02	R

R Large residual

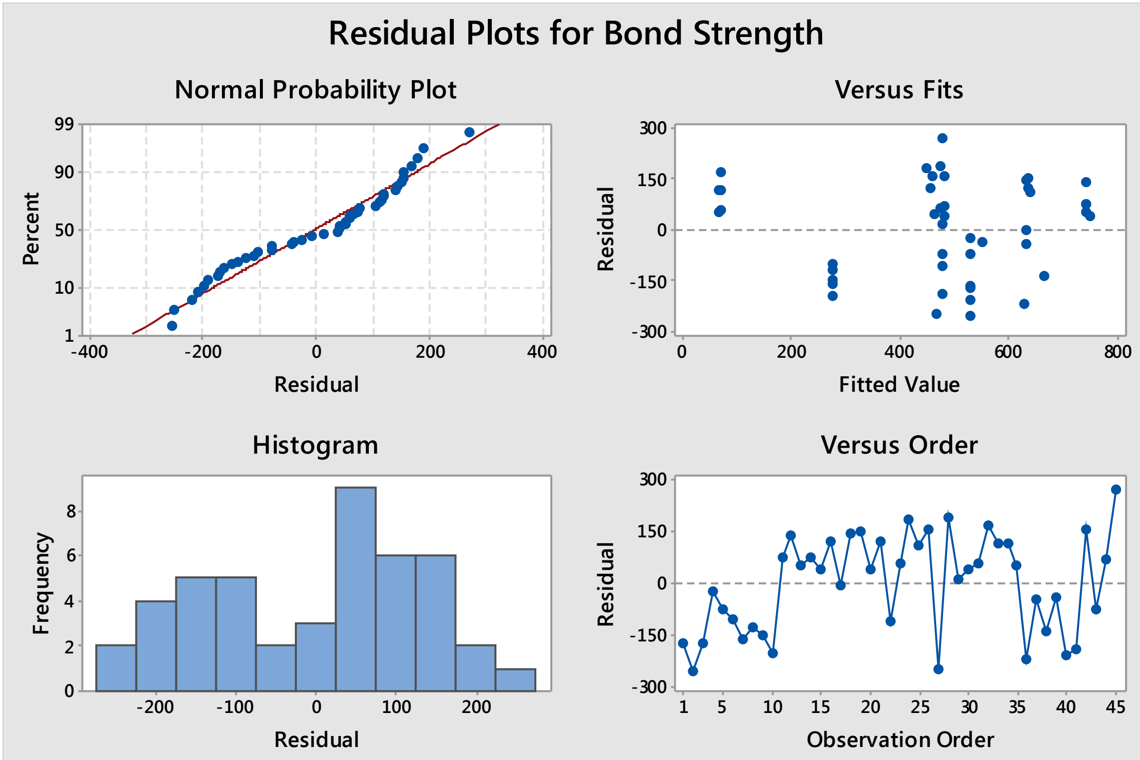
Residual Plots for Bond Strength
Normal Probability Plot
Percent
Residual
Versus Fits
Residual
Fitted Value
Histogram
Frequency
Residual
Versus Order
Residual
Observation Order

BIBLIOGRAPHY

Ahn, D., Kweon, J. H., Kwon, S., Song, J., & Lee, S. (2009). Representation of surface roughness in fused deposition modeling. Journal of Materials Processing Technology, 209(15), 5593-5600.

Alhubail, M. (2012). *Statistical-based optimization of process parameters of fused deposition modelling for improved quality* (Doctoral dissertation, University of Portsmouth).

Anitha, R., Arunachalam, S., & Radhakrishnan, P. (2001). Critical parameters influencing the quality of prototypes in fused deposition modelling. *Journal of Materials Processing Technology*, *118*(1), 385-388.

Brockmann, W., Geiß, P. L., Klingen, J., Schröder, B., & Mikhail, B. (2009). Adhesive bonding.

Budhe, S., Ghumatkar, A., Birajdar, N., & Banea, M. D. (2015). Effect of surface roughness using different adherend materials on the adhesive bond strength. *Applied Adhesion Science*, *3*(1), 1.

Christiyan, K. J., Chandrasekhar, U., & Venkateswarlu, K. (2016, February). A study on the influence of process parameters on the Mechanical Properties of 3D printed ABS composite. In *IOP Conference Series: Materials Science and Engineering* (Vol. 114, No. 1, p. 012109). IOP Publishing.

Cubberly, W. H. (1989). *Tool and Manufacturing Engineers Handbook Desk Edition*. Society of Manufacturing Engineers.

Fatimatuzahraa, A. W., Farahaina, B., & Yusoff, W. Y. (2011, September). The effect of employing different raster orientations on the mechanical properties and microstructure of Fused Deposition Modeling parts. In*Business, Engineering and Industrial Applications (ISBEIA), 2011 IEEE Symposium on* (pp. 22-27). IEEE.

Gao, W., Zhang, Y., Nazzetta, D. C., Ramani, K., & Cipra, R. J. (2015, November). RevoMaker: Enabling Multi-directional and Functionally-embedded 3D printing using a Rotational Cuboidal Platform. In *Proceedings of the 28th Annual ACM Symposium on User Interface Software & Technology* (pp. 437-446). ACM.

Grutle, Ø. K. (2015). 5-axis 3D Printer.

Grover, M. P., & Groover, M. P. (2012). *Fundamentals of Modern Manufacturing:* Materials, Processes, and Systems.

Gurrala, P. K., & Regalla, S. P. Prediction of Neck Growth due to Inter and Intra-Layer Bonding for High Strength Parts in Additive Manufacturing (AM).

Keating, S., & Oxman, N. (2013). Compound fabrication: A multi-functional robotic platform for digital design and fabrication. *Robotics and Computer-Integrated Manufacturing*, *29*(6), 439-448.

Krassenstein, E. (2014, July 24). MIT Researchers Create a ‘Smart’ 3D Printer That Can Locate an Object & Print on Top of it. Retrieved June 09, 2016, from 3dprint.com: https://3dprint.com/9952/mit-researchers-smart-3d-printer/

Krolczyk, G., Raos, P., & Legutko, S. (2014). Experimental analysis of surface roughness and surface texture of machined and fused deposition modelled parts. *Tehnički vjesnik*, *21*(1), 217-221.

Li, L., Sun, Q., Bellehumeur, C., & Gu, P. (2002, August). Investigation of bond formation in FDM process. In *Solid Freeform Fabrication Symp., Austin, TX* (pp. 1-8).

N. Turner, B., Strong, R., & A. Gold, S. (2014). A review of melt extrusion additive manufacturing processes: I. Process design and modeling. *Rapid Prototyping Journal*, *20*(3), 192-204.

Oropallo, W., & Piegl, L. A. (2016). Ten challenges in 3D printing.*Engineering with Computers*, *32*(1), 135-148.

Pan, A., Huang, Z., Guo, R., & Liu, J. (2016). Effect of FDM Process on Adhesive Strength of Polylactic Acid (PLA) Filament. *Key Engineering Materials*, *667*.

Piazza, M., & Alexander, S. (2015). Additive Manufacturing: A Summary of the Literature.

Song, X., Pan, Y., & Chen, Y. (2015). Development of a low-cost parallel kinematic machine for multidirectional additive manufacturing. Journal of Manufacturing Science and Engineering, 137(2), 021005.

Sood, A. K., Ohdar, R. K., & Mahapatra, S. S. (2009). Improving dimensional accuracy of fused deposition modelling processed part using grey Taguchi method. *Materials & Design*, *30*(10), 4243-4252.

Sreedhar, P., MathikumarManikandan, C., & Jothi, G. (2012). Experimental investigation of surface roughness for fused deposition modeled part with different angular orientation. *Technology, 5*(3), 21-28.

Sun, Q., Rizvi, G. M., Bellehumeur, C. T., & Gu, P. (2008). Effect of processing conditions on the bonding quality of FDM polymer filaments.*Rapid Prototyping Journal*, *14*(2), 72-80.

Teibrich, A., Mueller, S., Guimbretière, F., Kovacs, R., Neubert, S., & Baudisch, P. (2015, November). Patching Physical Objects. In *Proceedings of the 28th Annual ACM Symposium on User Interface Software & Technology* (pp. 83-91). ACM.

Udroiu, R., & Mihail, L. (2009, December). Experimental determination of surface roughness of parts obtained by rapid prototyping. In *8th WSEAS International Conference on Circuits, Systems, Electronics, Control and Signal Processing, Puerto De La Cruz, Tenerife, Canary Islands, Spain* (pp. 283-286).

Vasudevarao, B., Natarajan, D. P., Henderson, M., & Razdan, A. (2000, August). Sensitivity of RP surface finish to process parameter variation. In*Solid freeform fabrication proceedings* (pp. 251-258).

Wegman, R. F., & Van Twisk, J. (2012). *Surface preparation techniques for adhesive bonding*. William Andrew.

Zhang, Y., & Chou, Y. K. (2006). A parametric study of part distortions in FDM using 3D FEA. In *Proceedings of the 17th Solid Freeform Fabrication Symposium, Austin, TX, USA.*